
Optimal-speed unitary quantum time evolutions and propagation of light with maximal degree of coherence

Carlo Cafaro¹, Shannon Ray², and Paul M. Alsing²

¹*SUNY Polytechnic Institute, 12203 Albany, New York, USA and*

²*Air Force Research Laboratory, Information Directorate, 13441 Rome, New York, USA*

It is recognized that Grover arrived at his original quantum search algorithm inspired by his comprehension of the interference of classical waves originating from an array of antennae. It is also known that quantum-mechanical characterization of electromagnetic radiation is isomorphic to the treatment of the orientation of a spin-1/2 particle. In this paper, motivated by Grover's original intuition and starting from this mathematical equivalence, we present a quantitative link between the geometry of time-independent optimal-speed Hamiltonian evolutions on the Bloch sphere and the geometry of intensity-preserving propagation of light with maximal degree of coherence on the Poincaré sphere. Finally, identifying interference as the fundamental physical ingredient underlying both physical phenomena, we propose that our work can provide in retrospect a quantitative geometric background underlying Grover's powerful intuition.

PACS numbers: Quantum computation (03.67.Lx), Quantum information (03.67.Ac), Quantum mechanics (03.65.-w).

I. INTRODUCTION

It is known that the quantum-mechanical treatment of photon polarization is mathematically equivalent to the treatment of the orientation of a spin-1/2 particle [1]. In particular, focusing on the physics of two-level quantum systems and classical polarization optics in two-dimensions, the concepts of Bloch vector and Bloch sphere [2] are the analogues of the notions of Stokes vector and Poincaré sphere [3], respectively.

A remarkable link between quantum mechanics and classical optics is represented by the interpretation of Pancharatnam's optical phase that appears in the context of interference of polarized light [4] as an early example of Berry's (nondynamical) geometric phase that emerges in the context of cyclic and adiabatic quantum mechanical evolutions [5]. In classical optics, Pancharatnam's phase is the emergence of a phase shift in the state of polarization of a light beam during a cyclic change of the state [4]. Specifically, considering a beam of light that comes back to its original state of polarization via two intermediate polarizations, Pancharatnam showed that the phase does not return to its original value. Instead, it increases by $-\Omega/2$ with Ω being the solid angle spanned on the Poincaré sphere by the geodesic triangle whose vertices represent the three polarizations. For a simple proof of Pancharatnam's main result, we refer to Ref. [6]. In quantum mechanics, Berry's phase is the emergence of a geometric phase (over and above the dynamical phase) in the state of a quantum system during its adiabatic and cyclic unitary evolution. Specifically, if the system is in an eigenstate of the instantaneous Hamiltonian and the Hamiltonian returns to its initial state, the system also does, but it gains a geometric phase. For an in-depth discussion on the relation between Pancharatnam's phase and Berry's phase, we refer to Refs. [7, 8]. The work in Ref. [7] is especially illuminating since Berry, starting from the description of polarization in terms of the Poincaré sphere, expresses Pancharatnam's classical optics analysis in quantum mechanical language and, moreover, clarifies the relation between the classical optical phase and the quantum adiabatic phase. Interestingly, this mutual interaction between quantum mechanics and classical optics has been rather beneficial in science. For example, borrowing ideas from Pancharatnam's work on the classical interference of polarized light, Samuel and Bhandari extended the concept of Berry's phase to nonunitary and noncyclic quantum mechanical evolutions in Ref. [8]. Furthermore, just as Pancharatnam's theory was tested in an experimental fashion with the detection of the predicted phase shifts by interference, the first experimental manifestation of Berry's phase was carried out in an optical experiment [9] where the Berry phase measured corresponded to an angle of rotation of a plane of polarization of light [10]. A second close similarity between quantum mechanics and classical optics is the correspondence between the degree of polarization of beams of light and the parity of qubits as reported in Refs. [11, 12]. The origin of this similarity can be explained as follows. In the quantum mechanical Bloch sphere formalism, the origin represents a maximally mixed state, whereas points on the surface of the sphere are pure states. In the Poincaré sphere formalism in classical optics, the origin represents a completely unpolarized light beam, whereas points on the surface of the sphere are completely polarized beams.

In quantum mechanics, there are several ways in which one can derive an expression of time-independent optimal-speed Hamiltonians evolving an initial state $|A\rangle$ into a final state $|B\rangle$. For instance, a simple derivation can rely on finding Hamiltonians $\{H\}$ that evolve $|A\rangle$ into $|B\rangle$ in the least time subject to the constraint that the difference between the largest and the smallest eigenvalues of H is held fixed [13]. Another straightforward derivation, instead,

can put the emphasis on choosing the Hamiltonian so that the uncertainty in energy is maximized [14]. In any case, the trajectories connecting $|A\rangle$ and $|B\rangle$ generated by such optimal-speed unitary evolutions $\{U\}$ can be viewed as geodesic curves on the Bloch sphere (or, alternatively, the two-sphere S^2). For this reason, it is especially interesting the geometric interpretation of these unitary operators $\{U\}$ with $|A\rangle \xrightarrow{U} |B\rangle$ in terms of rotations of the Bloch sphere around the axis that is orthogonal to the hemispherical plane containing the origin along with $|A\rangle$ and $|B\rangle$. In particular, the Hamiltonian that generates the rotation takes the form $H = E_+ |E_+\rangle \langle E_+| + E_- |E_-\rangle \langle E_-|$ for a pair of real parameters E_{\pm} with the axis of rotation corresponding to a pair of orthogonal states $|E_{\pm}\rangle$ [15, 16]. More generally, given that the dynamics induced by a optimal-speed unitary evolution can be regarded as a rigid rotation of the two-sphere S^2 , if there exists a unitary evolution transforming $|A\rangle$ into $|B\rangle$ with $\langle A|B\rangle = 0$ along a geodesic path, then there must exist a pair of energy eigenstates $|E_+\rangle$ and $|E_-\rangle$, say at the equator of S^2 , such that $|A\rangle$ and $|B\rangle$ lie at the poles of S^2 [17]. Moreover, in terms of an efficiency measure defined by means of the ratio between the distance along the shortest geodesic path joining $|A\rangle$ and $|B\rangle$ and the distance along the actual dynamical trajectory traced by the state vector $|\psi(t)\rangle \stackrel{\text{def}}{=} e^{-\frac{i}{\hbar}Ht}|A\rangle$, these optimal-speed unitary quantum mechanical evolutions exhibit unit “*quantum geometric efficiency*” [18, 19].

In classical polarization optics, it is known that the degree of polarization of a light wave propagating along the \hat{z} -direction does not depend on the choice of the \hat{x} - and \hat{y} -directions. Furthermore, such a degree of polarization is an upper bound for the so-called degree of coherence between the electric vibrations in the \hat{x} - and \hat{y} -directions [3]. Interestingly, it can be demonstrated that there always exists a pair of orthogonal directions for which the degree of coherence has its maximum value and this value is equal to the degree of polarization of the light wave [20]. Therefore, considering the ratio between the degree of coherence and the degree of polarization as some sort of “*classical optical efficiency*”, it happens that there is always an optimal optical configuration in which the propagation of polarized light occurs with maximal degree of coherence.

In this paper, we wish to investigate an unexplored link between optimal-speed quantum mechanical evolutions and propagation of light with maximal degree of coherence. Our investigation is inspired by the above mentioned existing links between quantum mechanics and classical optics. Furthermore, we rely on our familiarity with both digital and analog quantum search algorithms [19, 21–25]. In addition, our proposed investigation finds additional motivation by recalling that Grover’s original intuition that helped him creating his quantum search algorithm [26] was based upon a classical optics phenomenon. Specifically, Grover arrived at his quantum search algorithm by observing the interference of classical waves originating from an array of antennae [27]. This way, by mimicking the interference of *classical* waves, Grover arrived at his *quantum* search scheme.

Therefore, motivated by this intriguing similarity between the existence of a convenient pair of orthogonal energy eigenstates in the geometrical description of optimal-speed quantum evolutions and the existence of a suitable pair of orthogonal directions for the electric field in the geometric description of propagation of polarized light with optimal-coherence, we provide in this paper a quantitative link between quantum mechanics and classical polarization optics. Specifically, starting from the mathematical equivalence between the quantum-mechanical characterization of electromagnetic radiation and the treatment of the orientation of a spin-1/2 particle, we discuss in a quantitative manner the connection between the geometry of time-independent optimal-speed Hamiltonian evolutions on the Bloch sphere and the geometry of intensity-preserving propagation of light with maximal degree of coherence on the Poincaré sphere. Identifying interference as the essential physical ingredient underlying both phenomena being studied in our paper, we conclude by arguing that our work can provide a quantitative geometric background underlying Grover’s powerful intuition.

The layout of the remainder of this paper is as follows. In Section II, we discuss two alternative characterizations of optimal-speed Hamiltonians. The first analysis focuses on minimizing the evolution time subject to the energy eigenvalue constraint. The second one, instead, relies on the maximization of the energy uncertainty that yields the spectral decomposition of the optimal Hamiltonian. We conclude Section II with a discussion on unit geometric efficiency on the Bloch sphere. In Section III, after providing some motivational background, we characterize the propagation of light in terms of the polarization ellipse, the Stokes parameters, and the Poincaré sphere. Then, we briefly present the concepts of coherence of electric vibrations along with degree of coherence, coherency matrix, and degree of polarization of a light wave. In Section IV, we discuss the propagation of polarized light with maximal degree of coherence, that is propagation of light with unit optical efficiency on the Poincaré sphere. The quantitative link between the geometry of time-independent optimal-speed Hamiltonian evolutions on the Bloch sphere and the geometry of intensity-preserving propagation of light with maximal degree of coherence on the Poincaré sphere is carried out throughout Sections II and IV. In Section V, we discuss the physical origin of our proposed link. Our concluding remarks appear in Section VI. A number of technical details and remarks appear in Appendices A, B, C, and D. Specifically, in Appendix A we place some specific properties of the Mueller matrices in optics. In this Appendix B, we employ the Poincaré sphere formalism to describe the dependence of the modulus of the complex degree of coherence of a partially polarized light beam in terms of the ellipticity and orientation angles. In this Appendix C,

we report some mathematical details on the parametrization of qubits and polarization states regarded as points on the Bloch sphere and the Poincaré sphere, respectively. Finally, we present in Appendix D a discussion on the role played by interference effects in light propagation, quantum searching, and optimal-speed quantum evolutions.

II. QUANTUM EVOLUTIONS WITH UNIT GEOMETRIC EFFICIENCY

In this section, we discuss two alternative descriptions of optimal-speed Hamiltonians. The first characterization focuses on minimizing the evolution time subject to the energy eigenvalue constraint. The second one, instead, depends on the maximization of the energy uncertainty that leads to the spectral decomposition of the optimal Hamiltonian. We conclude this section with a discussion on unit geometric efficiency on the Bloch sphere.

When studying the geometric characterization of unit efficiency [18] quantum mechanical unitary evolutions specified by time-independent Hamiltonians $\{H\}$ under which a normalized initial state vector $|A\rangle$ evolves into a normalized final state vector $|B\rangle$, one notices at least two alternative approaches in the literature. In a first approach, researchers aim to find an expression of the Hamiltonian by minimizing the evolution time $\Delta t \stackrel{\text{def}}{=} T_{AB}$ needed for evolving $|A\rangle$ into $|B\rangle$ subject to the constraint that the difference between the largest (E_+) and smallest (E_-) eigenvalues of the Hamiltonian is kept fixed [13], $E_+ - E_- \stackrel{\text{def}}{=} E_0 = \text{fixed}$. In a second approach, instead, investigators seek for an expression of the Hamiltonian by maximizing the uncertainty in energy ΔE of the system [14]. This approach is motivated by the fact that the (angular) speed of evolution v of the quantum system is proportional to ΔE , $v \stackrel{\text{def}}{=} ds_{\text{FS}}/dt \propto \Delta E$, with s_{FS} denoting the Fubini-Study distance between the two points on the projective Hilbert space $\mathcal{P}(\mathcal{H})$ that corresponds to the selected initial and final states $|A\rangle$ and $|B\rangle$, respectively. Despite the fact that these two quantum approaches are essentially equivalent since the constraint on the difference between the largest and the smallest eigenvalues of the Hamiltonian is similar to upper bounding the energy uncertainty ΔE since $\Delta E_{\text{max}} = (E_+ - E_-)/2$, they do put the emphasis on distinct features that will help us better understanding the details of the optimal evolution Hamiltonian. Ultimately, these complementary features will help us describing the formal analogies between the geometry of quantum evolutions with unit quantum geometric efficiency and the geometry of classical polarization optics for light waves with degree of polarization P that equals the degree of coherence $|j_{xy}|$ between the electric vibrations in any two mutually orthogonal directions of propagation of the wave [20]. Unit quantum geometric efficiency means here that $\eta_{\text{QM}} \stackrel{\text{def}}{=} s_0/s = 1$, where s_0 is the distance along the shortest geodesic joining the initial and final points of the evolution that are distinct on the projective Hilbert space while s is the distance along the effective evolution of the system in the projective Hilbert space as measured by the Fubini-Study metric. Finally, unit classical optical efficiency means here $\eta_{\text{optics}} \stackrel{\text{def}}{=} |j_{xy}|/P = 1$.

A. Minimizing the evolution time

The starting point of the first approach can be summarized as follows. Given a time-independent Hamiltonian H with a corresponding unitary time-evolution operator $U(t) \stackrel{\text{def}}{=} e^{-\frac{i}{\hbar}Ht}$, one wishes to evolve a state $|A\rangle$ into a state $|B\rangle$ in the shortest possible time subject to the constraint that the difference $E_+ - E_-$ between the largest (E_+) and the smallest (E_-) eigenvalues of H is kept fixed. In summary, we wish to find the optimal Hamiltonian acting in the two-dimensional subspace spanned by $|A\rangle$ and $|B\rangle$ that yields the optimal time evolution subject to the constraint $E_+ - E_- \stackrel{\text{def}}{=} E_0 = \text{fixed}$.

We begin by considering the following unitary evolution scheme,

$$|A\rangle = \begin{pmatrix} \alpha_1 \\ \alpha_2 \end{pmatrix} \xrightarrow{e^{-\frac{i}{\hbar}Ht}} |B\rangle = \begin{pmatrix} \beta_1 \\ \beta_2 \end{pmatrix}, \text{ with } H \stackrel{\text{def}}{=} \begin{pmatrix} h_{11} & h_{12}e^{-i\phi} \\ h_{12}e^{i\phi} & h_{22} \end{pmatrix} \quad (1)$$

and, where h_{11} , h_{12} , h_{22} , and ϕ are four real quantities. We assume that $|A\rangle$ and $|B\rangle$ are normalized to one so that $|\alpha_1|^2 + |\alpha_2|^2 = 1$ and $|\beta_1|^2 + |\beta_2|^2 = 1$. The spectral decomposition of H in Eq. (1) can be recast as $H = E_+ |E_+\rangle\langle E_+| + E_- |E_-\rangle\langle E_-|$ with the energy eigenvalue constraint given by,

$$(E_+ - E_-)^2 = (h_{11} - h_{22})^2 + 4h_{12}^2 = \text{constant} \stackrel{\text{def}}{=} E_0^2. \quad (2)$$

In view of our interest in studying the action of $e^{-\frac{i}{\hbar}Ht}$ onto $|A\rangle$, it is convenient to observe that H in Eq. (1) can be decomposed in terms of the Pauli matrices $\vec{\sigma} \stackrel{\text{def}}{=} (\sigma_x, \sigma_y, \sigma_z)$ as

$$H = \frac{h_{11} + h_{22}}{2} I + \frac{E_0}{2} \hat{a} \cdot \vec{\sigma}. \quad (3)$$

In Eq. (3), I denotes the identity matrix while $\hat{a} \stackrel{\text{def}}{=} \vec{a}/\|\vec{a}\|$ with $\|\vec{a}\| = E_0/2$ is a unit vector defined as,

$$\hat{a} \stackrel{\text{def}}{=} \frac{2}{E_0} \left(h_{12} \cos(\phi), h_{12} \sin(\phi), \frac{h_{11} - h_{22}}{2} \right). \quad (4)$$

We emphasize at this stage that finding the optimal evolution Hamiltonian reduces to finding the optimal set of the four real parameters $\{h_{11}, h_{12}, h_{22}, \phi\}$ in Eq. (1) or, equivalently, the optimal \hat{a} that appears in Eq. (3). Using Eq. (3) along with algebraic manipulations that are typical in quantum mechanics with Pauli matrices, the action of $e^{-\frac{i}{\hbar}Ht}$ onto $|A\rangle$ leading to the state $|B\rangle$ in a time T_{AB} yields

$$\begin{pmatrix} \beta_1 \\ \beta_2 \end{pmatrix} = e^{-\frac{i}{\hbar} \frac{h_{11}+h_{22}}{2} T_{AB}} \left(\alpha_1 \begin{bmatrix} \cos\left(\frac{E_0}{2\hbar} T_{AB}\right) - i \frac{h_{11}-h_{22}}{E_0} \sin\left(\frac{E_0}{2\hbar} T_{AB}\right) \\ -ie^{i\phi} \frac{2h_{12}}{E_0} \sin\left(\frac{E_0}{2\hbar} T_{AB}\right) \end{bmatrix} + \alpha_2 \begin{bmatrix} -ie^{-i\phi} \frac{2h_{12}}{E_0} \sin\left(\frac{E_0}{2\hbar} T_{AB}\right) \\ \cos\left(\frac{E_0}{2\hbar} T_{AB}\right) + i \frac{h_{11}-h_{22}}{E_0} \sin\left(\frac{E_0}{2\hbar} T_{AB}\right) \end{bmatrix} \right). \quad (5)$$

At this point, we note that the components of the states $|A\rangle$ and $|B\rangle$ depend on the choice of the basis of the two-dimensional subspace spanned by these two vectors. Therefore, for the sake of computational simplicity and without loss of generality, we choose a basis so that $|A\rangle = (1, 0)$ and $|B\rangle = (\alpha, \beta)$. With this choice, Eq. (5) reduces to

$$\begin{pmatrix} \alpha \\ \beta \end{pmatrix} = e^{-\frac{i}{\hbar} \frac{h_{11}+h_{22}}{2} T_{AB}} \begin{pmatrix} \cos\left(\frac{E_0}{2\hbar} T_{AB}\right) - i \frac{h_{11}-h_{22}}{E_0} \sin\left(\frac{E_0}{2\hbar} T_{AB}\right) \\ -ie^{i\phi} \frac{2h_{12}}{E_0} \sin\left(\frac{E_0}{2\hbar} T_{AB}\right) \end{pmatrix}. \quad (6)$$

Considering the modulus of β as expressed in Eq. (6), we note that the expression of the evolution time T_{AB} becomes

$$T_{AB} = \frac{2\hbar}{E_0} \sin^{-1} \left(\frac{E_0 |\beta|}{2h_{12}} \right). \quad (7)$$

We observe that the $\sin^{-1}(x)$ function is a monotonic increasing function of its argument x with $\sin^{-1}(0) = 0$. Therefore, since E_0 and $|\beta|$ are held fixed, the minimum value of T_{AB} in Eq. (7) is reached when h_{12} assumes its maximum possible value. The maximum possible value h_{12}^{max} of h_{12} compatible with the eigenvalue constraint in Eq. (2) is reached when $h_{11} = h_{22}$ and equals $h_{12}^{\text{max}} = E_0/2$. Therefore, the optimal evolution time $T_{AB}^{\text{min}} = T_{AB}(h_{12}^{\text{max}})$ is equal to

$$T_{AB}^{\text{min}} = \frac{2\hbar}{E_0} \sin^{-1}(|\beta|), \quad (8)$$

or, equivalently, $T_{AB}^{\text{min}} = (2\hbar/E_0) \cos^{-1}(|\alpha|)$ using the normalization condition $|\alpha|^2 + |\beta|^2 = 1$ along with properties of the $\sin^{-1}(x)$ function. So far, we have realized that the optimal set of the four real parameters $\{h_{11}, h_{12}, h_{22}, \phi\}$ is specified by $h_{12}^{\text{max}} = E_0/2$ and $h_{11} = h_{22}$. Therefore, it remains to find the explicit expressions for the optimal h_{11} and ϕ . These expressions can be found as follows. Let us set $\alpha \stackrel{\text{def}}{=} |\alpha| e^{i\varphi_\alpha}$ and $\beta \stackrel{\text{def}}{=} |\beta| e^{i\varphi_\beta}$ with φ_α and φ_β in \mathbb{R} . Inserting Eq. (8) into Eq. (6), we obtain

$$\begin{pmatrix} |\alpha| e^{i\varphi_\alpha} \\ |\beta| e^{i\varphi_\beta} \end{pmatrix} = e^{-\frac{i}{\hbar} h_{11} T_{AB}^{\text{min}}} \begin{pmatrix} \sqrt{1 - |\beta|^2} \\ -ie^{i\phi} |\beta| \end{pmatrix}. \quad (9)$$

With the help of some algebra, Eq. (9) yields

$$h_{11} = -\frac{\omega_0}{2} \frac{\varphi_\alpha}{\sin^{-1}(|\beta|)}, \text{ and } \phi = \varphi_\beta - \varphi_\alpha + \frac{\pi}{2}. \quad (10)$$

In conclusion, recalling the $h_{12}^{\text{max}} = E_0/2$ and $h_{11} = h_{22}$ together with Eq. (10), the optimal evolution Hamiltonian can be recast as [28]

$$H = \frac{E_0}{2} \begin{pmatrix} \frac{\varphi_\alpha}{\sin^{-1}(|\beta|)} & e^{-i(\varphi_\beta - \varphi_\alpha - \frac{\pi}{2})} \\ e^{i(\varphi_\beta - \varphi_\alpha - \frac{\pi}{2})} & \frac{\varphi_\alpha}{\sin^{-1}(|\beta|)} \end{pmatrix}. \quad (11)$$

Interestingly, we note that the expectation value of the Hamiltonian $\langle A|H|A\rangle$ is equal to $(\varphi_\alpha E_0)/2 \sin^{-1}(|\beta|)$ while the energy uncertainty of H in Eq. (11) is given by $\Delta E \stackrel{\text{def}}{=} \left[\langle A|H^2|A\rangle - \langle A|H|A\rangle^2 \right]^{1/2} = E_0/2$. Using the energy eigenvalue

constraint in Eq. (2), we also notice that $\Delta E = (E_+ - E_-)/2$. As a final remark, we point out that since overall phases of state vectors have unobservable effects in quantum mechanics, the Hamiltonians H and $H - (1/2)\text{tr}(H)I$ assume an identical maximal value ΔE_{\max} of energy uncertainty ΔE . Therefore, despite having different expectation values, these Hamiltonians generate the same physics of quantum evolutions. For this reason, for example, one may set the phase φ_α in Eq.(11) equal to zero.

Starting from a traceless Hamiltonian with $\Delta E_{\max} = (E_+ - E_-)/2$ will be the starting point in the second approach to optimal quantum evolutions that we treat in our paper. This second approach is based upon maximizing the energy uncertainty rather than minimizing the time evolution and will be discussed in the next subsection.

B. Maximizing the energy uncertainty

The starting point of the second approach can be summarized as follows. Consider a time-independent and traceless Hamiltonian H with a spectral decomposition given by $H = E_- |E_- \rangle \langle E_-| + E_+ |E_+ \rangle \langle E_+|$, where $E_+ \geq E_-$ and $\langle E_+ | E_- \rangle = \delta_{+, -}$. One wishes to evolve a state (not necessarily normalized) $|A\rangle$ into a state $|B\rangle$ in the shortest possible time by maximizing the energy uncertainty $\Delta E \stackrel{\text{def}}{=} \left[\langle A | H^2 | A \rangle / \langle A | A \rangle - (\langle A | H | A \rangle / \langle A | A \rangle)^2 \right]^{1/2}$ and obtain $\Delta E = \Delta E_{\max}$.

For the sake of simplicity, we denote $|E_\pm\rangle = |E_{2,1}\rangle$ and $E_\pm = E_{2,1}$ in what follows. To find the value of ΔE_{\max} , we note that an arbitrary unnormalized initial state $|A\rangle$ can be decomposed as $|A\rangle = \alpha_1 |E_1\rangle + \alpha_2 |E_2\rangle$ with $\alpha_1, \alpha_2 \in \mathbb{C}$. Then, after some algebra, we get

$$\Delta E = \frac{E_2 - E_1}{2} \left[1 - \left(\frac{|\alpha_1|^2 - |\alpha_2|^2}{|\alpha_1|^2 + |\alpha_2|^2} \right)^2 \right]^{1/2}. \quad (12)$$

From Eq. (12), we note that the maximum value of ΔE is obtained for $|\alpha_1| = |\alpha_2|$ (with α_1 and α_2 given by $\langle E_1 | A \rangle$ and $\langle E_2 | A \rangle$, respectively) and equals $\Delta E_{\max} \stackrel{\text{def}}{=} (E_2 - E_1)/2$ as mentioned in the previous subsection. The main underlying idea in this second approach is that of recasting $H = E_1 |E_1\rangle \langle E_1| + E_2 |E_2\rangle \langle E_2|$ in terms of the initial and final states $|A\rangle$ and $|B\rangle$ while keeping,

$$\Delta E = \Delta E_{\max} \stackrel{\text{def}}{=} \frac{E_2 - E_1}{2}. \quad (13)$$

Observe that in terms of the eigenvectors of the Hamiltonian, $|A\rangle$ and $|B\rangle$ can be decomposed as $|A\rangle = \alpha_1 |E_1\rangle + \alpha_2 |E_2\rangle$, and $|B\rangle = \beta_1 |E_1\rangle + \beta_2 |E_2\rangle$, respectively. To ensure minimum travel time T_{AB}^{\min} (that is, $\Delta E = \Delta E_{\max}$), we need to set $|\alpha_1| = |\alpha_2|$ and $|\beta_1| = |\beta_2|$. Therefore, let $\alpha_2 = e^{i\varphi_\alpha} \alpha_1$ and $\beta_2 = e^{i\varphi_\beta} \beta_1$ with $\varphi_{\alpha,\beta} \in \mathbb{R}$. Then, $|A\rangle$ and $|B\rangle$ become

$$|A\rangle = \alpha_1 |E_1\rangle + \alpha_2 |E_2\rangle = \alpha_1 |E_1\rangle + e^{i\varphi_\alpha} \alpha_1 |E_2\rangle, \quad (14)$$

and,

$$|B\rangle = \beta_1 |E_1\rangle + \beta_2 |E_2\rangle = \beta_1 |E_1\rangle + e^{i\varphi_\beta} \beta_1 |E_2\rangle, \quad (15)$$

respectively. From Eqs. (14) and (15), we obtain $|E_1\rangle + e^{i\varphi_\alpha} |E_2\rangle = \alpha_1^{-1} |A\rangle \stackrel{\text{def}}{=} \sqrt{2} |A\rangle$ and $|E_1\rangle + e^{i\varphi_\beta} |E_2\rangle = \beta_1^{-1} |B\rangle \stackrel{\text{def}}{=} \sqrt{2} e^{-i\frac{\varphi_\alpha - \varphi_\beta}{2}} |B\rangle$. After some matrix algebra, we get

$$\begin{pmatrix} |E_1\rangle \\ |E_2\rangle \end{pmatrix} = \frac{\sqrt{2}}{e^{i\frac{\varphi_\alpha + \varphi_\beta}{2}} - e^{i\varphi_\alpha} e^{i\frac{\varphi_\alpha - \varphi_\beta}{2}}} \begin{pmatrix} e^{i\frac{\varphi_\alpha + \varphi_\beta}{2}} & -e^{i\varphi_\alpha} \\ -e^{i\frac{\varphi_\alpha - \varphi_\beta}{2}} & 1 \end{pmatrix} \begin{pmatrix} \frac{\alpha_1^{-1}}{\sqrt{2}} |A\rangle \\ \frac{\beta_1^{-1}}{\sqrt{2}} e^{i\frac{\varphi_\alpha - \varphi_\beta}{2}} |B\rangle \end{pmatrix}. \quad (16)$$

For the sake of completeness, we emphasize that

$$|\langle A | B \rangle|^2 = \frac{|\langle A | B \rangle|^2}{\langle A | A \rangle \langle B | B \rangle} = \cos^2 \left(\frac{\varphi_\alpha - \varphi_\beta}{2} \right) = \cos^2 \left(\frac{\theta}{2} \right), \quad (17)$$

with $\theta \stackrel{\text{def}}{=}} \varphi_\alpha - \varphi_\beta = 2s_{\text{FS}} = s_{\text{geo}}$ where s_{FS} and s_{geo} denote the Fubini-Study and the geodesic distances, respectively. Finally, using Eq. (16) along with noting that $E_2 = -E_1 \stackrel{\text{def}}{=} E$ since the Hamiltonian is assumed to be traceless, we

obtain after some simple but tedious algebra that the spectral decomposition $H = E_1 |E_1\rangle \langle E_1| + E_2 |E_2\rangle \langle E_2|$ becomes [29]

$$H = \frac{iE}{\sin\left(\frac{\varphi_\alpha - \varphi_\beta}{2}\right)} [|\mathcal{B}\rangle \langle \mathcal{A}| - |\mathcal{A}\rangle \langle \mathcal{B}|]. \quad (18)$$

In terms of the original initial and final states $|A\rangle$ and $|B\rangle$, after some additional simple but laborious algebra, the Hamiltonian in Eq. (18) can be finally recast as

$$H = iE \cot\left(\frac{\varphi_\alpha - \varphi_\beta}{2}\right) \left[\frac{|B\rangle \langle A|}{\langle A|B\rangle} - \frac{|A\rangle \langle B|}{\langle B|A\rangle} \right], \quad (19)$$

while the geodesic line $|\psi(t)\rangle = e^{-\frac{i}{\hbar}Ht} |A\rangle$ with H in Eq. (19) connecting the two states $|A\rangle$ and $|B\rangle$ can be written as

$$|\psi(t)\rangle = \left[\cos\left(\frac{E}{\hbar}t\right) - \frac{\cos\left(\frac{\varphi_\alpha - \varphi_\beta}{2}\right)}{\sin\left(\frac{\varphi_\alpha - \varphi_\beta}{2}\right)} \sin\left(\frac{E}{\hbar}t\right) \right] |A\rangle + \frac{e^{i\frac{\varphi_\alpha - \varphi_\beta}{2}}}{\sin\left(\frac{\varphi_\alpha - \varphi_\beta}{2}\right)} \sin\left(\frac{E}{\hbar}t\right) |B\rangle, \quad (20)$$

where $0 \leq t \leq T_{AB}^{\min}$ with $T_{AB}^{\min} = \hbar\theta / (2E)$. For the sake of completeness, we note that for H in Eq. (19), we correctly get $\langle A|H|A\rangle / \langle A|A\rangle = 0$ and $\Delta E = [\langle A|H^2|A\rangle / \langle A|A\rangle]^{1/2} = E = \Delta E_{\max}$. In conclusion, the Hamiltonians in Eqs. (11) and (19) are optimal-speed Hamiltonians yielding unit quantum geometric efficiency $\eta_{QM} = 1$.

Having discussed in detail the two main constructions of Hamiltonians yielding unit quantum geometric efficiency, in the next section we focus on the geometric characterization of the propagation of polarized light with maximal degree of coherence. As we present this classical optics description, we will emphasize analogies and determine exactly correspondences with the above mentioned quantum mechanical characterizations.

III. PROPAGATION OF POLARIZED LIGHT AND DEGREE OF COHERENCE

In this section, we describe the propagation of light by means of the polarization ellipse, the Stokes parameters, and the Poincaré sphere. Then, we briefly define the notions of coherence of electric vibrations, degree of coherence, coherency matrix, and degree of polarization of a light wave. We end this section with a discussion on propagation of polarized light with maximal degree of coherence, that is, unit classical optical efficiency on the Poincaré sphere. However, before beginning with our formal descriptions, we present some motivational background that helps explaining our underlying motivations for presenting this material of polarization optics.

A. Motivational background

Two important quantities in optics when studying the physics of polarized light are the degree of polarization P of the wave and the degree of coherence $|j_{xy}|$ of the electric vibrations. The quantity P is defined as [3],

$$P \stackrel{\text{def}}{=} \frac{I_{\text{pol}}}{I_{\text{tot}}}, \quad (21)$$

with $I_{\text{tot}} \stackrel{\text{def}}{=} I_{\text{pol}} + I_{\text{unpol}}$ denoting the total intensity of the wave and I_{pol} being the intensity of the monochromatic (hence, polarized) part of the wave. The quantity P with $0 \leq P \leq 1$ expresses the ‘‘amount of polarization’’ present in the wave. In particular, the wave is completely unpolarized when $P = 0$ and completely polarized when $P = 1$. When $0 < P < 1$, the light is partially polarized. The degree of coherence $|j_{xy}|$, instead, is defined as the modulus of the complex degree of coherence j_{xy} [3],

$$j_{xy} \stackrel{\text{def}}{=} \frac{J_{xy}}{\sqrt{J_{xx}}\sqrt{J_{yy}}}. \quad (22)$$

In Eq. (22), $J_{ij} \stackrel{\text{def}}{=} \langle E_i(t) E_j^*(t) \rangle$ are the matrix coefficients of the so-called coherency matrix J and the sharp brackets denote the time average operation. The quantity $|j_{xy}|$ with $0 \leq |j_{xy}| \leq |j_{xy}|_{\max}$, instead, measures the

Bloch Sphere	Polarization Ellipse	Poincare Spheré
$(A\rangle, A_{\perp}\rangle)$	$(\hat{\xi}, \hat{\eta})$	\vec{S}_{initial}
$(E_{+}\rangle_{\text{sub-optimal}}, E_{-}\rangle_{\text{sub-optimal}})$	(\hat{x}, \hat{y})	$\vec{S}_{\text{sub-optimal}}$
$(E_{+}\rangle_{\text{optimal}}, E_{-}\rangle_{\text{optimal}})$	(\hat{x}', \hat{y}')	\vec{S}_{optimal}
$\mathcal{H} = a_0 I + \vec{a} \cdot \vec{\sigma}$	\vec{E}	$J = \frac{1}{2} \vec{S} \cdot \vec{\sigma}$
$\hat{a} = \hat{a}(\theta, \varphi)$	$\vec{E} = \vec{E}(\beta, \chi)$	$\vec{S} = \vec{S}(2\beta, 2\chi)$
$e^{-i \frac{\ \vec{a}\ T_{AB}}{\hbar} \hat{a} \cdot \vec{\sigma}}$	$R_{\hat{z}}(\alpha)$	$\text{MROT}(\alpha)$
s_0 , fixed	\vec{E} , fixed	P , fixed
$s(0) \rightarrow s(T_{AB})$	$[\vec{E}]_{\{\hat{x}, \hat{y}\}} \rightarrow [\vec{E}]_{\{\hat{x}', \hat{y}'\}}$	$ j_{xy}\rangle \rightarrow j_{x'y'}\rangle$
$\eta_{\text{QM}} \stackrel{\text{def}}{=} s_0/s$	$\langle E_x E_x^* \rangle - \langle E_y E_y^* \rangle$	$\eta_{\text{optics}} \stackrel{\text{def}}{=} j_{xy} /P$

TABLE I: Schematic depiction of the most relevant quantities that specify optimal-speed unitary quantum time evolutions on the Bloch sphere together with the analogue quantities that characterize the propagation of light with maximal degree of coherence by means of the polarization ellipse and the Poincaré sphere representations of polarized light.

degree of correlation of the electric vibrations. When $|j_{xy}| = 0$, the electric vibrations are uncorrelated and do not give rise to any interference effect. In this case, the vibrations may be said to be incoherent. When $|j_{xy}| = |j_{xy}|_{\text{max}}$, the vibrations may be said to be coherent. Finally, when $0 < |j_{xy}| < |j_{xy}|_{\text{max}}$, vibrations are known as partially coherent. The quantity P can be fully expressed in terms of the determinant and the trace of the coherency matrix J as shown in Ref. [3]. Therefore, it is a quantity whose value does not change under arbitrary rotations of the orthogonal Cartesian axes used to describe the electric vibrations. However, unlike the degree of polarization of the wave, the degree of coherence $|j_{xy}|$ between the electric vibrations in any two mutually orthogonal directions of propagation of the wave is generally affected by the specific choice of the two orthogonal directions [3]. In particular, it is possible to show that there always exist a pair of orthogonal directions for which the degree of coherence $|j_{xy}|$ of the electric vibrations reaches its maximum value $|j_{xy}|_{\text{max}}$ and, in addition, this value equals the degree of polarization P of the wave [20]. Interestingly, this particular pair of orthogonal directions has a clear geometrical interpretation. Indeed, representing the wave as an incoherent mixture of a wave of natural radiation and a wave of monochromatic (hence, completely polarized) radiation, it can be shown that these directions for which the degree of coherence $|j_{xy}|$ equals the degree of polarization P are the bisectors of the principal directions (that is, major and minor axes) of the polarization ellipse of the polarized portion of the wave [30].

The existence of a pair of directions (\hat{x}', \hat{y}') rotated around the \hat{z} -axis (that is, the axis that specifies the direction of propagation of the wave) by a specific angle φ_{opt} that affects the electric vibrations in such a manner that the quantity $\eta_{\text{opt}} \stackrel{\text{def}}{=} |j_{xy}|/P$, that we name *classical optical efficiency* in this paper, equals one is reminiscent of the existence of a pair of orthogonal states $(|E_{+}\rangle, |E_{-}\rangle)$ that defines the axis of rotation of the Bloch sphere orthogonal to the hemispherical plane containing the initial and final unit states $|A\rangle$ and $|B\rangle$ as discussed in the previous section. In the quantum case, this rotation around the $\hat{n}_{E_{+}}$ -axis by an angle $2 \cos^{-1} [|\langle A|B\rangle|]$ is essentially the unitary evolution operator emerging from the optimal-speed Hamiltonian that yields efficiency $\eta_{\text{QM}} \stackrel{\text{def}}{=} s_0/s$ equal to one. Furthermore, just as these directions (\hat{x}', \hat{y}') for which $|j_{xy}| = P$ are the bisectors of the principal directions $(\hat{\xi}, \hat{\eta})$ corresponding to the major and minor axes, respectively, of the polarization ellipse, in a similar fashion, the pair of orthogonal states $(|E_{+}\rangle, |E_{-}\rangle)$ for which $s_0 = s$ lie in the equatorial plane when the pair of states $(|A\rangle, |A_{\perp}\rangle)$ are assumed to lie at the poles. Finally, the angle φ_{opt} seems to be replaced in the quantum case by the azimuthal angle $\varphi_{E_{+}}$ that serves to specify the location of $|E_{+}\rangle$ on the Bloch sphere. We shall devote the rest of this paper to make these formal analogies as quantitative as possible. We shall begin by observing that to better characterize the propagation of the effects of this simple two-dimensional rotation of the canonical Cartesian axes (\hat{x}, \hat{y}) on the electric vibrations along with the coherency matrix J and, ultimately, on the degree of coherence $|j_{xy}|$, we need to better understand how to visualize and perform calculations when considering polarized light. For this reason, we shall introduce the concepts of polarization ellipse along with that of the Poincaré sphere.

To better motivate the definitions and concepts of polarization optics in what follows, we present in Table I a schematic depiction of the most relevant quantities that specify optimal-speed unitary quantum time evolutions on the Bloch sphere together with the analogue quantities that characterize the propagation of light with maximal degree of coherence by means of the polarization ellipse and the Poincaré sphere representations of polarized light. Clearly, these correspondences will become more transparent as we go through the next subsections and Section IV.

B. Polarization of a light wave

In the previous section, we have explained how the Hamiltonian operator affects the path of evolution of a quantum system (specifically, a spin-1/2 particle) in terms of geometric evolutions on a Bloch sphere. In this section, keeping the directions of rays of light constant during its propagation, we focus on the state of polarization and the intensity of the light as it passes through an optical system. In this case, the three fundamental types of optical elements are wave plates, rotators, and polarizers. These elements give rise to phase shifting, rotations, and anisotropic attenuation, respectively. More specifically, we are interested here in intensity-preserving linear optical transformations which quantify the effect of rotators on polarized light in a geometric fashion. For such a quantification, we need to arrive at the Poincaré sphere description of polarized light. The way we plan to pursue this goal can be outlined as follows. Firstly, we begin with the polarization ellipse representation of polarized light [3]. Secondly, we introduce the Stokes parameters from the polarization ellipse [31]. Finally, we introduce the Poincaré sphere by attaching a geometric interpretation to the Stokes parameters [32]. We remark that the traditional language for studying the two-component electric vector of the light is the so-called Jones-matrix formalism based upon the use of 2×2 complex matrices [33]. Alternatively, regarding the Stokes parameters as the components of a column matrix or 4-vector and optical devices as represented by 4×4 matrices [34], the so-called Mueller matrix method can be employed to quantify the effect of optical devices on polarized light. For further details on the Mueller matrices in optics, we refer to Appendix A.

Polarization ellipse. Assume that the electric vector field \vec{E} of the light propagating along the \hat{z} -axis is given by $\vec{E} = E_x(t)\hat{x} + E_y(t)\hat{y}$ with $E_x(t)$ and $E_y(t)$ defined as $E_x(t) \stackrel{\text{def}}{=} E_{0x}(t) \cos[\omega t + \delta_x(t)]$ and $E_y(t) \stackrel{\text{def}}{=} E_{0y}(t) \cos[\omega t + \delta_y(t)]$, respectively. The quantities ω , $\delta_x(t)$, and $\delta_y(t)$ specify the plane wave and denote the instantaneous angular frequency and the two instantaneous phases, respectively. After some algebraic manipulations of the two relations involving $E_x(t)$ and $E_y(t)$, one arrives at an equation of an ellipse in a nonstandard form given by

$$\frac{E_x^2(t)}{E_{0x}^2(t)} + \frac{E_y^2(t)}{E_{0y}^2(t)} - \frac{2E_x(t)E_y(t)}{E_{0x}(t)E_{0y}(t)} \cos[\delta(t)] = \sin^2[\delta(t)], \quad (23)$$

with $\delta \stackrel{\text{def}}{=} \delta_x - \delta_y$ [31]. The ellipse defined by Eq. (23) is not in its standard form since $E_x(t)$ and $E_y(t)$ are not directed along the \hat{x} - and \hat{y} -axes. Instead, they are directed along the $\hat{\xi}$ - and $\hat{\eta}$ -directions obtained from the canonical Cartesian axes via a rotation around the \hat{z} -axis by an angle χ . This angle is known as the orientation angle with $0 \leq \chi < \pi$ and, clearly, it describes how tilted is the ellipse with respect to the canonical Cartesian axes. For the sake of completeness and later use, we also introduce at this point the so-called ellipticity angle β with $-\pi/4 < \beta \leq \pi/4$ defined as $\tan \beta \stackrel{\text{def}}{=} b/a$ with a and b being the major and minor axes of the polarization ellipse, respectively. This angle specifies the shape of the ellipse. In what follows, we introduce the Stokes parameters from the polarization ellipse.

The Stokes parameters from the polarization ellipse. Focusing on monochromatic radiation with E_{0x} , E_{0y} , δ_x , and δ_y constant in time, Eq. (23) reduces to

$$\frac{E_x^2(t)}{E_{0x}^2} + \frac{E_y^2(t)}{E_{0y}^2} - \frac{2E_x(t)E_y(t)}{E_{0x}E_{0y}} \cos \delta = \sin^2 \delta. \quad (24)$$

To represent Eq. (24) in terms of observables of the electromagnetic radiation, one needs to consider a time average over an infinite time interval. However, given the periodic behavior of $E_x(t)$ and $E_y(t)$, averaging over a single period of vibration T will suffice. Specifically, define the time average of $E_i(t)E_j(t)$ as

$$\langle E_i(t)E_j(t) \rangle \stackrel{\text{def}}{=} \frac{1}{T} \int_0^T E_i(t)E_j(t) dt. \quad (25)$$

Using Eq. (25), it can be shown following Ref. [31] that the time-averaged version of Eq. (24) can be recast as

$$S_0^2 = S_1^2 + S_2^2 + S_3^2, \quad (26)$$

with $S_0 \stackrel{\text{def}}{=} E_{0x}^2 + E_{0y}^2$, $S_1 \stackrel{\text{def}}{=} E_{0x}^2 - E_{0y}^2$, $S_2 \stackrel{\text{def}}{=} 2E_{0x}E_{0y} \cos \delta$, and $S_3 \stackrel{\text{def}}{=} 2E_{0x}E_{0y} \sin \delta$. The four parameters $\{S_i\}$ with $0 \leq i \leq 3$ are the observables of the polarization ellipse with S_0 being the total intensity of the radiation while $\{S_1, S_2, S_3\}$ specify the state of polarization of the light beam. These are the so-called four Stokes polarization parameters [35]. Eq. (26) holds for completely polarized light and S_0 is redundant in this case. Instead, for partially polarized light, $S_0^2 \geq S_1^2 + S_2^2 + S_3^2$ and S_0 is no longer redundant. The excess $S_0^2 - (S_1^2 + S_2^2 + S_3^2)$ indicates the amount

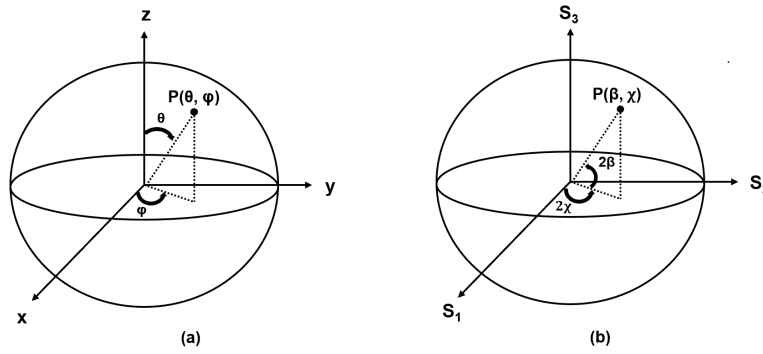


FIG. 1: In (a), we depict the Bloch sphere for pure quantum states of a single qubit. A point $P = P(\theta, \varphi)$ on the surface of the Bloch sphere is defined by the Bloch vector $\vec{r} \stackrel{\text{def}}{=} (r_x, r_y, r_z) = (r \sin \theta \cos \varphi, r \sin \theta \sin \varphi, r \cos \theta)$ with $\|\vec{r}\| = 1$. Mixed states are specified by $\|\vec{r}\| \leq 1$, with the origin representing a maximally mixed state. The angles θ and φ are the polar and the azimuthal angles, respectively. In (b), we depict the Poincaré sphere of unit radius for the polarized state of a beam of light. A point $P = P(\beta, \chi)$ on the surface of the Poincaré sphere is defined by the vector $\vec{s} \stackrel{\text{def}}{=} (S_1, S_2, S_3) = (S_0 \cos 2\beta \cos 2\chi, S_0 \cos 2\beta \sin 2\chi, S_0 \sin 2\beta)$ where $\vec{S} \stackrel{\text{def}}{=} (S_0, S_1, S_2, S_3)$ with $S_1^2 + S_2^2 + S_3^2 = S_0^2 \equiv 1$ is the Stokes vector specified by the four Stokes parameters $\{S_0, S_1, S_2, S_3\}$. The parameter S_0 denotes the total intensity of the beam while the remaining three parameters S_1, S_2 and, S_3 specify the polarization state of the beam. A partially polarized beam of light is specified by $S_0 \leq 1$, with the origin being a completely unpolarized beam. Finally, β and χ are the ellipticity and the orientation angles, respectively.

of unpolarized light present in the beam. More specifically, for completely polarized light beams, $S_0 \stackrel{\text{def}}{=} I_{\text{tot}} = I_{\text{pol}}$. Instead, for partially polarized light, $S_0 \stackrel{\text{def}}{=} I_{\text{tot}} > I_{\text{pol}}$. We refer to Appendix B for details on the behavior of $|j_{xy}|$ for partially polarized waves using the Poincaré sphere formalism.

In what follows, we introduce the Poincaré sphere by attaching a geometric interpretation to the Stokes parameters.

The Poincaré sphere from the Stokes parameters. It can be verified by a straightforward but tedious computation as mentioned in Refs. [32, 36] that for a fixed value of S_0 , we have for completely polarized light $S_1 \stackrel{\text{def}}{=} S_0 \cos(2\beta) \cos(2\chi)$, $S_2 \stackrel{\text{def}}{=} S_0 \cos(2\beta) \sin(2\chi)$, and $S_3 \stackrel{\text{def}}{=} S_0 \sin(2\beta)$ with β and χ being the ellipticity and orientation angles, respectively, as previously defined. Setting $S_0 = 1$, the quantities $\{S_1, S_2, S_3\}$ have the following geometric interpretation. Consider the vector $\vec{s} \stackrel{\text{def}}{=} (S_1, S_2, S_3)$ with length $\|\vec{s}\| = S_0 = 1$. The vector \vec{s} is located on a sphere of unit length with its location determined by the azimuth angle 2χ and the latitude angle 2β . Thus, a beam of elliptically polarized light can be specified by the vector \vec{s} as mapped on the sphere as originally pointed out by Poincaré in Ref. [37]. For a graphical depiction of the Bloch and Poincaré spheres, we refer to Fig. 1. For more details on the parametrization of qubits and polarization states viewed as points on the Bloch sphere and the Poincaré sphere, respectively, we refer to Appendix C.

C. Coherence of the electric vibrations

Having discussed the basics of polarized light, in this subsection we present the essentials concerning the notion of coherence of the electric vibrations.

Given the electric vector of the incident light wave in its complex form, the so-called coherency matrix J is defined as [20],

$$J = \begin{pmatrix} J_{xx} & J_{xy} \\ J_{yx} & J_{yy} \end{pmatrix} \stackrel{\text{def}}{=} \begin{pmatrix} \langle E_x E_x^* \rangle & \langle E_x E_y^* \rangle \\ \langle E_y E_x^* \rangle & \langle E_y E_y^* \rangle \end{pmatrix}, \quad (27)$$

where the sharp brackets denote time average. The coherency matrix J is an Hermitian matrix with $J_{xy}^* = J_{yx}$ and characterizes the incident wave. In particular, $\text{tr}(J)$ represents the intensity of the incident wave and its off-diagonal coefficients describe the correlation between the x - and y -components of \vec{E} . We observe that employing the Schwarz inequality for integrals, it follows that $|J_{xy}| \leq \sqrt{J_{xx}} \sqrt{J_{yy}}$ and $|J_{yx}| \leq \sqrt{J_{yy}} \sqrt{J_{xx}}$. Therefore, $\det(J) \stackrel{\text{def}}{=} J_{xx} J_{yy} - J_{xy} J_{yx} \geq 0$. The Stokes parameters can be expressed in terms of the coherency matrix coefficients by the relations $S_0 \stackrel{\text{def}}{=} J_{xx} + J_{yy}$, $S_1 \stackrel{\text{def}}{=} J_{xx} - J_{yy}$, $S_2 \stackrel{\text{def}}{=} J_{xy} + J_{yx}$, and $S_3 \stackrel{\text{def}}{=} i(J_{yx} - J_{xy})$. Inverting these equations, one

gets $J_{xx} = (S_0 + S_1)/2$, $J_{yy} = (S_0 - S_1)/2$, $J_{xy} = (S_2 + iS_3)/2$, and $J_{yx} = (S_2 - iS_3)/2$. Therefore, the relation between the Stokes parameters $\{S_0, S_1, S_2, S_3\}$ and the coherency matrix J can be recast in the following compact form [1, 20],

$$J = \frac{1}{2} \sum_{i=0}^3 S_i \sigma_i, \quad (28)$$

where in Eq. (28) $\sigma_0 = I_{2 \times 2}$, $\sigma_1 = \sigma_z$, $\sigma_2 = \sigma_x$, $\sigma_3 = -\sigma_y$ with $\{\sigma_x, \sigma_y, \sigma_z\}$ being the usual Pauli spin matrices in quantum mechanics. To quantify the electric vibrations in the \hat{x} - and \hat{y} -directions, we introduce the so-called complex degree of coherence

$$j_{xy} = |j_{xy}| e^{i\beta_{xy}} \stackrel{\text{def}}{=} \frac{J_{xy}}{\sqrt{J_{xx}} \sqrt{J_{yy}}}. \quad (29)$$

In Eq. (29), $|j_{xy}|$ is the modulus of the complex degree of coherence (we shall call it, degree of coherence) and measures the degree of correlation of the vibrations. The phase $\beta_{xy} \in \mathbb{R}$, instead, specifies the effective phase difference between the vibrations. As a side remark, we note that $\det(J) \geq 0$ implies $|j_{xy}| \leq 1$. We notice that J in Eq. (27) will change if the \hat{x} - and \hat{y} -axes are rotated about the direction of propagation of the wave. Therefore, since $|j_{xy}|$ is not expressed in terms of rotation-invariant terms, it depends on the choice of the \hat{x} - and \hat{y} -axes. Unlike $|j_{xy}|$, the degree of polarization P in Eq. (21) of a wave can be expressed in terms of rotation-invariant quantities built from the coherency matrix as we shall see in the next subsection.

D. Degree of polarization and coherency matrix

To express the degree of polarization of a wave in terms of the coherency matrix, we proceed as follows. Recall that a general coherency matrix J_{general} can be formally recast as,

$$J_{\text{general}} = \begin{pmatrix} J_{xx} & J_{xy} \\ J_{yx} & J_{yy} \end{pmatrix} \stackrel{\text{def}}{=} \begin{pmatrix} \alpha_1 & \gamma_1 - i\delta_1 \\ \gamma_1 + i\delta_1 & \beta_1 \end{pmatrix}, \quad (30)$$

with $\alpha_1, \beta_1, \gamma_1, \delta_1 \in \mathbb{R}$. Moreover, recall that any wave can be represented as a superposition of a wave of natural radiation with coherency matrix $J_{\text{natural}} \stackrel{\text{def}}{=} [D^2, 0; 0, D^2]$ and a completely elliptically polarized (monochromatic) wave with coherency matrix $J_{\text{pol}} \stackrel{\text{def}}{=} [A^2, -iAB; iAB, B^2]$ with $A, B, D \in \mathbb{R}$. Then, it can be shown that all light is a case or limiting case of partially elliptically polarized light with coherency matrix given by $J_{\text{tot}} \stackrel{\text{def}}{=} J_{\text{natural}} + J_{\text{pol}}$,

$$J_{\text{tot}} = \begin{pmatrix} A^2 + D^2 & -iAB \\ iAB & B^2 + D^2 \end{pmatrix}. \quad (31)$$

To prove this statement, it is sufficient to show there exists a transformation that allows us to set Eq. (31) equal to Eq. (30). Indeed, it turns out that $J_{\text{tot}} = T(\chi) \cdot J_{\text{general}} \cdot T^{-1}(\chi)$ where $T(\chi) \stackrel{\text{def}}{=} [\cos \chi, \sin \chi; \sin \chi, -\cos \chi]$ is a real unitary transformation with χ being the angle (that is, the orientation angle for the polarization ellipse that corresponds to the light beam) defined by the condition [38],

$$\tan(2\chi) = \frac{2\gamma_1}{\alpha_1 - \beta_1} = \frac{J_{xy} + J_{yx}}{J_{xx} - J_{yy}}. \quad (32)$$

For further details on how to express A , B , and D in terms of $\alpha_1, \beta_1, \gamma_1, \delta_1$, we refer to Ref. [38]. Now, setting $J_{xx} \stackrel{\text{def}}{=} A^2 + D^2$, $J_{xy} \stackrel{\text{def}}{=} -iAB$, $J_{yx} \stackrel{\text{def}}{=} iAB$, and $J_{yy} \stackrel{\text{def}}{=} B^2 + D^2$, we finally have

$$P \stackrel{\text{def}}{=} \frac{I_{\text{pol}}}{I_{\text{tot}}} = \frac{\text{tr}(J_{\text{pol}})}{\text{tr}(J_{\text{tot}})} = \left[1 - \frac{4 \det(J_{\text{tot}})}{[\text{tr}(J_{\text{tot}})]^2} \right]^{1/2}. \quad (33)$$

From Eq. (33), we note that P does not depend on the choice of the \hat{x} - and \hat{y} -directions. Furthermore, from Eq. (33) and the definition of $|j_{xy}|$, we obtain after some algebra that $|j_{xy}| \leq P$ [20]. The equality $|j_{xy}| = P$ holds iff $J_{xx} = J_{yy}$. It can be shown that a pair of orthogonal directions \hat{x}' and \hat{y}' always exist for which this is the case.

The fact that $|j_{xy}|$ depends on the choice of the \hat{x} and \hat{y} directions while P does not, along with the definition of the angle χ in Eq. (32), will play a major role in our discussion of unit optical efficiency in the next section.

Type of Sphere	Constraint Description	Constraint Equation
Bloch	bounded energy of the system	$(E_+ - E_-)^2 = (h_{11} - h_{22})^2 + 4h_{12}h_{21} = \text{fixed}$
Bloch	maximal energy dispersion	$\Delta E = \Delta E_{\text{max}}$, and $\Delta t = \Delta t_{\text{min}}$
Poincaré	bounded intensity of light	$I_{\text{pol}}^2 = (J_{xx} - J_{yy})^2 + 4J_{xy}J_{yx} = \text{fixed}$
Poincaré	maximal correlations between E_x and E_y	$S_2^2 = (S_2^2)_{\text{max}}$, and $S_1^2 = 0$

TABLE II: Schematic summary of the main constraint equations yielding unit efficiency geodesic paths on the Bloch sphere and optical paths leading to polarization states with maximal degree of coherence on the Poincaré sphere.

IV. PROPAGATION OF LIGHT WITH UNIT OPTICAL EFFICIENCY

In this section, we finally describe the propagation of polarized light with maximal degree of coherence.

Let us define a measure of optical efficiency as the ratio between the degree of polarization of the wave and the degree of coherence of the electric vibrations, $\eta_{\text{opt}} \stackrel{\text{def}}{=} |j_{xy}|/P$. This quantity achieves its maximum value 1 when $|j_{xy}| = P$, that is to say, when $J_{xx} = J_{yy}$. For a fixed value of P or, analogously, for a fixed value of $I_{\text{pol}} \stackrel{\text{def}}{=} \text{tr}(J_{\text{pol}}) = \left[(J_{xx} + J_{yy})^2 + 4 \det(J_{\text{pol}}) \right]^{1/2} = \text{constant}$ [20], we wish to find a new pair of orthogonal directions $\{\hat{x}', \hat{y}'\}$ such that $J_{x'x'} = J_{y'y'}$ and, consequently, $\eta_{\text{opt}} = 1$. First, using the definition of $\det(J_{\text{tot}})$, we note that the constraint on I_{pol} can be recast as

$$I_{\text{pol}}^2 = (J_{xx} - J_{yy})^2 + 4J_{xy}J_{yx} = \text{constant}. \quad (34)$$

Therefore, from Eq. (34) we have that the optimal coherency matrix J' is specified by $J_{x'x'} = J_{y'y'}$ and $|J_{x'y'}| = I_{\text{pol}}/2$. Observe that Eq. (34) is the analogue of Eq. (2). Furthermore, the quantum conditions $h_{11} = h_{22}$ and $h_{12}^{\text{max}} = E_0/2$ correspond to the optical conditions $J_{x'x'} = J_{y'y'}$ and $|J_{x'y'}| = I_{\text{pol}}/2$, respectively.

Alternatively, in terms of the Stokes vector components, unit optical efficiency demands

$$S_1^2 \rightarrow (S_1^2)_{\text{min}} = 0, \text{ with } S_2^2 \rightarrow (S_2^2)_{\text{max}}. \quad (35)$$

Note that the minimization of S_1^2 and the maximization of S_2^2 correspond to the minimization of the evolution time and the maximization of the energy uncertainty, respectively. In Table II, we present a schematic of the main constraint equations yielding unit efficiency geodesic paths on the Bloch sphere (that is, Eqs. (2) and (13)) and optical paths leading to polarization states with maximal degree of coherence on the Poincaré sphere (that is, Eqs. (34) and (35)).

To find the pair of orthogonal directions $\{\hat{x}', \hat{y}'\}$, we assume they are obtained from the canonical Cartesian directions $\{\hat{x}, \hat{y}\}$ via a rotation $R_{\hat{z}}(\varphi_{\text{opt}}) \stackrel{\text{def}}{=} [\cos \varphi_{\text{opt}}, \sin \varphi_{\text{opt}}; -\sin \varphi_{\text{opt}}, \cos \varphi_{\text{opt}}]$ around the \hat{z} -axis by an angle φ_{opt} to be determined. Specifically, the components of the electric field \vec{E} with respect to the basis $\{\hat{x}', \hat{y}'\}$ satisfy

$$\left[\vec{E} \right]_{\{\hat{x}, \hat{y}\}} \rightarrow \left[\vec{E} \right]_{\{\hat{x}', \hat{y}'\}} \stackrel{\text{def}}{=} R_{\hat{z}}(\varphi_{\text{opt}}) \cdot \left[\vec{E} \right]_{\{\hat{x}, \hat{y}\}}. \quad (36)$$

The transformation laws for the coherency matrix and the Stokes vector emerging from Eq. (36) are given by [39],

$$J \rightarrow J' \stackrel{\text{def}}{=} R_{\hat{z}}(\varphi_{\text{opt}}) \cdot J \cdot R_{\hat{z}}(-\varphi_{\text{opt}}), \quad (37)$$

and [40],

$$S \rightarrow S' \stackrel{\text{def}}{=} M_{\text{ROT}}(\varphi_{\text{opt}}) S = \mathcal{U} \cdot [R_{\hat{z}}^*(\varphi_{\text{opt}}) \otimes R_{\hat{z}}(\varphi_{\text{opt}})] \cdot \mathcal{U}^\dagger, \quad (38)$$

respectively, where \mathcal{U} is a (4×4) -unitary matrix and $M_{\text{ROT}}(\varphi_{\text{opt}})$ is a (4×4) - Mueller matrix given by

$$\mathcal{U} \stackrel{\text{def}}{=} \frac{1}{\sqrt{2}} \begin{pmatrix} 1 & 0 & 0 & 1 \\ 1 & 0 & 0 & -1 \\ 0 & 1 & 1 & 0 \\ 0 & i & -i & 0 \end{pmatrix}, \text{ and } M_{\text{ROT}}(\varphi_{\text{opt}}) \stackrel{\text{def}}{=} \begin{pmatrix} 1 & 0 & 0 & 0 \\ 0 & \cos(2\varphi_{\text{opt}}) & \sin(2\varphi_{\text{opt}}) & 0 \\ 0 & -\sin(2\varphi_{\text{opt}}) & \cos(2\varphi_{\text{opt}}) & 0 \\ 0 & 0 & 0 & 1 \end{pmatrix}, \quad (39)$$

respectively. Imposing that $J_{x'x'} = J_{y'y'}$, from Eq. (37) we get that φ_{opt} is such that

$$\tan(2\varphi_{\text{opt}}) = \frac{J_{yy} - J_{xx}}{J_{xy} + J_{yx}}. \quad (40)$$

Quantity of Interest	Bloch Sphere	Poincaré Sphere
angles	(θ, φ)	(β, χ)
range of angles	$0 \leq \theta \leq \pi, 0 \leq \varphi < 2\pi$	$-\pi/4 < \beta \leq \pi/4, 0 \leq \chi < \pi$
point on the sphere	$P(\theta, \varphi) \stackrel{\text{def}}{=} (\sin \theta \cos \varphi, \sin \theta \sin \varphi, \cos \theta)$	$P(\beta, \chi) \stackrel{\text{def}}{=} (\cos 2\beta \cos 2\chi, \cos 2\beta \sin 2\chi, \sin 2\beta)$
axis of rotation	$\hat{E}_+ = \hat{E}_+(\theta_{E_+}, \varphi_{E_+})$	\hat{z} , fixed
angle of rotation	$\cos^{-1} [\langle A B \rangle]$, fixed	φ_{opt}
angles to be compared	$\varphi_{E_+} = \varphi_{E_+}(A\rangle, B\rangle)$	$\varphi_{\text{opt}} = \varphi_{\text{opt}}(P)$, with $P = P(\beta, \chi)$

TABLE III: Schematic description of quantities of interest on the Bloch and the Poincaré spheres. In particular, we compare the description of points $P(\theta, \varphi)$ and $P(\beta, \chi)$ on the two surfaces in terms of their spherical coordinates. Moreover, we describe the rotation operations yielding unit efficiency on the two spheres in terms of their axes of rotation (that is, \hat{E}_+ and \hat{z} , respectively) and their angles of rotation (that is, $\cos^{-1} [|\langle A|B \rangle|]$ and φ_{opt} , respectively). Finally, we identify the two angles φ_{E_+} and φ_{opt} to be compared within the two geometric frameworks of unit efficiency quantum evolutions and polarization optics.

Since J_{xx} , J_{yy} , and $J_{xy} + J_{yx} = 2 \text{Re}(J_{xy}) \in \mathbb{R}$, Eq. (40) has a real root. In conclusion, there always exists a pair of orthogonal directions $\{\hat{x}', \hat{y}'\}$ with $\hat{x}' \stackrel{\text{def}}{=} \hat{x} \cos \varphi_{\text{opt}} + \hat{y} \sin \varphi_{\text{opt}}$ and $\hat{y}' \stackrel{\text{def}}{=} -\hat{x} \sin \varphi_{\text{opt}} + \hat{y} \cos \varphi_{\text{opt}}$ for which the two intensities J_{xx} and J_{yy} are equal. For this pair of directions, the degree of coherence $|j_{xy}|$ reaches its maximum value $|j_{xy}|_{\text{max}}$ with $|j_{xy}|_{\text{max}} = P$. This particular pair of directions $\{\hat{x}', \hat{y}'\}$ has a neat geometric interpretation. Indeed, using Eqs. (32) and (40), it follows that

$$\tan(2\varphi_{\text{opt}}) \tan(2\chi) = -1, \quad (41)$$

that is, $\varphi_{\text{opt}} - \chi = \pi/4$ or $3\pi/4$. Therefore, the directions $\{\hat{x}', \hat{y}'\}$ for which $\eta_{\text{opt}} \stackrel{\text{def}}{=} |j_{xy}|/P = 1$ are the bisectors of the principal directions $\{\hat{\xi}, \hat{\eta}\}$ with $\hat{\xi} \stackrel{\text{def}}{=} \hat{x} \cos \chi + \hat{y} \sin \chi$ and $\hat{\eta} \stackrel{\text{def}}{=} -\hat{x} \sin \chi + \hat{y} \cos \chi$ of the polarization ellipse of the polarized portion of the wave [20]. Therefore, given that $\hat{x}' = \hat{\xi} \cos(\varphi_{\text{opt}} - \chi) + \hat{\eta} \sin(\varphi_{\text{opt}} - \chi)$ and $\hat{y}' = -\hat{\xi} \sin(\varphi_{\text{opt}} - \chi) + \hat{\eta} \cos(\varphi_{\text{opt}} - \chi)$ with $\varphi_{\text{opt}} - \chi = \pi/4$ or $3\pi/4$, we have

$$\left| \hat{x}' \cdot \hat{\xi} \right| = \left| \hat{x}' \cdot \hat{\eta} \right| = \left| \hat{y}' \cdot \hat{\xi} \right| = \left| \hat{y}' \cdot \hat{\eta} \right| = 1/2, \quad (42)$$

since $\hat{x}' = (\hat{\xi} + \hat{\eta})/\sqrt{2}$ and $\hat{y}' = (\hat{\eta} - \hat{\xi})/\sqrt{2}$. Observe that the optical conditions in Eq. (42) correspond to the quantum conditions

$$|\langle E_+|A \rangle| = |\langle E_-|A \rangle| = |\langle E_+|A_\perp \rangle| = |\langle E_-|A_\perp \rangle| = 1/2, \quad (43)$$

obtained when maximizing the energy uncertainty in Eq. (12). In Table III, we provide a schematic description of quantities of interest on the Bloch and the Poincaré spheres. In particular, we characterize the points $P(\theta, \varphi)$ and $P(\beta, \chi)$ on the two surfaces in terms of their spherical coordinates. Moreover, we specify the rotation operations yielding unit efficiency on the two spheres by means of their axes of rotation (that is, \hat{E}_+ and \hat{z} , respectively) and their angles of rotation (that is, $\cos^{-1} [|\langle A|B \rangle|]$ and φ_{opt} , respectively). Finally, we determine the two angles φ_{E_+} and φ_{opt} to be compared within the two geometric frameworks of unit efficiency quantum evolutions and unit efficiency polarized light propagation.

In the next section, we discuss the physical root that is underlying our proposed formal analogy.

V. PHYSICAL ORIGIN BEHIND THE FORMAL ANALOGY

The formal analogy between quantum evolutions with unit geometric efficiency and propagation of light with unit optical efficiency, discussed in this paper and summarized in Tables I and II, is yet another example of the close relationship that exists between certain classes of quantum mechanical and classical optical phenomena. Is this analogy completely unexpected? What is the physical reason that underlines such a formal similarity? This analogy is not completely unexpected. After all, as mentioned in the Introduction, Grover exploited his knowledge on the interference of classical light waves in order to construct his quantum search algorithm. Furthermore, the set of unit-speed quantum mechanical evolutions includes as a special case the Farhi-Gutmann search Hamiltonian [41], an analog version of Grover's digital quantum search scheme. Both Grover's and the Farhi-Gutmann search schemes rely heavily on the interference phenomenon for achieving their quadratic speedup. The phenomenon of interference, either

constructive or destructive, plays a key role in both light propagation [38, 42] and quantum searching [43, 44]. For additional details on the role played by interference effects in light propagation, quantum searching, and optimal-speed quantum evolutions, we refer to Appendix D.

In what follows, we briefly discuss the role played by interference as the physical root underlying the formal analogy between propagation of light with maximal degree of coherence and optimal-speed unitary quantum propagation proposed in this paper.

A. Interference of classical light waves

In the framework of coherent light propagation [38], two rays of light originating from the same source can interfere. Specifically, the two rays can be combined in such a manner to give rise to a light more intense than is ordinarily created by two light beams of their respective intensities (constructive interference). Alternatively, the superimposition of the two rays of light can yield a darkness (destructive interference). Therefore, coherent light propagation is characterized by interference effects where, in addition, the degree of coherence is equal to the degree of indistinguishability of the particle trajectories that yield the interference pattern [42]. When the photon pattern becomes identifiable, the interference effects disappear, and the light propagation becomes incoherent. In the study of coherence properties of partially polarized electromagnetic radiation [20], there is a proper angle that specifies a pair of directions for which the degree of coherence of the electric vibrations has its maximum value (which, in turn, equals the degree of polarization of the wave). As discussed in this paper, this angle φ_{opt} is determined by a specific value of the orientation angle χ that characterizes the polarization ellipse used to describe the light propagation (see Eq. (41)).

From a more quantitative standpoint, consider a quasi-monochromatic light wave that propagates in the \hat{z} -direction specified by an electric field $\vec{E}(t) = E_x(t)\hat{x} + E_y(t)\hat{y}$. Assume that the component $E_\theta = \vec{E} \cdot \hat{\theta}$ of the electric field in the $\hat{\theta}$ -direction is given by, $E_\theta(t; \theta, \varepsilon) \stackrel{\text{def}}{=} E_x(t) \cos(\theta) + E_y e^{i\varepsilon} \sin(\theta)$, with ε denoting the phase delay between E_x and E_y . The interference law of light waves can be expressed by calculating the intensity $I(\theta, \varepsilon)$ of the light vibrations in the direction which makes an angle θ with the positive \hat{x} -direction. A straightforward calculation yields [20],

$$I(\theta, \varepsilon) = I_x + I_y + 2\sqrt{I_x}\sqrt{I_y}|j_{xy}|\cos(\beta_{xy} - \varepsilon). \quad (44)$$

In Eq. (44), $I(\theta, \varepsilon) \stackrel{\text{def}}{=} \langle E_\theta(t; \theta, \varepsilon) E_\theta^*(t; \theta, \varepsilon) \rangle$ where sharp brackets denote time average, $I_x \stackrel{\text{def}}{=} J_{xx} \cos^2(\theta)$, $I_y \stackrel{\text{def}}{=} J_{yy} \sin^2(\theta)$, J_{ij} are the coefficients of the coherency matrix, and $j_{xy} \stackrel{\text{def}}{=} |j_{xy}| e^{i\beta_{xy}}$ is the complex degree of coherence of the electric vibrations in the \hat{x} - and \hat{y} -directions. Recall that $|j_{xy}|$ in Eq. (44) is an indicator of the degree of correlation of the vibrations, while β_{xy} in Eq. (44) is an effective phase difference between the electric vibrations in the \hat{x} - and \hat{y} -directions. In modern terminology, we emphasize that J_{ij} are known as the coefficients of the polarization matrix [45]. Moreover, in the context of the classical theory of optical fluctuations and coherence, the analogue of $|j_{xy}|$ is the so-called degree of first order coherence [46]. Regardless of notation and modern terminology, what is most important for us here is the contribution of j_{xy} with the interference term $|j_{xy}|\cos(\beta_{xy} - \varepsilon)$ into the expression of the total intensity $I(\theta, \varepsilon)$ in Eq. (44).

Interestingly, when studying the superposition of two coherent beams of light in different states of elliptic polarization, Pancharatnam showed in Ref. [4] that if A and B represent the states of polarization on the Poincaré sphere of the given interfering beams, and C that of the resultant beam, the intensity of the resultant beam can be recast as

$$I_C = I_A + I_B + 2\sqrt{I_A}\sqrt{I_B} \cos\left(\frac{\theta_{AB}^{\text{Poincaré}}}{2}\right) \cos(\delta). \quad (45)$$

In Eq. (45), $\theta_{AB}^{\text{Poincaré}}$ is the angular separation of states A and B on the Poincaré sphere, while δ is not quite the absolute difference of phase between the two beams and is defined as the phase advance of the first beam being in a state of polarization A over the A -component of the second beam being in a state of polarization B . If we set $\varepsilon = \varepsilon_y$ in Eq. (44) and consider a nonvanishing phase ε_x , δ can be formally identified with $\varepsilon_x - (\varepsilon_y - \beta_{xy})$. For more details, we refer to Ref. [4].

B. Interference of quantum probability amplitudes

In the framework of quantum searching viewed in the context of quantum computing as multi-particle interference [43, 44], the role of interference is fundamental since it permits the evolution from a source state to a target state by manipulating the intermediate multi-particle superpositions in a convenient way. Specifically, quantum searching

can be regarded as inducing a proper relative phase between two eigenvectors to generate constructive interference on the searched elements and destructive interference on the remaining ones. As pointed out in this paper, this phase is quantified by a specific value of the azimuthal angle φ_{E_+} that specifies the location on the Bloch sphere of the eigenstates $|E_{\pm}\rangle$ used to geometrically construct the optimal evolution (search) Hamiltonian H .

Therefore, interference appears to be the essential physical phenomenon that underlies both propagation of light with maximal degree of coherence and continuous-time quantum search evolution with minimum search time (i.e., optimal-speed). Interference is optimally exploited in the two above mentioned tasks so that unit optical and quantum efficiencies can be achieved by identifying suitable angles. These are the orientation and azimuthal angles in the optical and quantum search cases, respectively. The orientation angle φ_{opt} specifies the optimal unitary operation (Mueller rotation, $M_{\text{ROT}}(\varphi_{\text{opt}})$) that connects the two initial and final polarization states on the Poincaré sphere. The azimuthal angle φ_{E_+} , instead, characterizes the optimal unitary operation (Bloch rotation, $R_{\hat{E}_+}(\theta_{AB})$ with $\theta_{AB} \stackrel{\text{def}}{=} \cos^{-1} [|\langle A|B\rangle|]$ and $\hat{E}_+ \stackrel{\text{def}}{=} \hat{E}_+(\theta_{E_+}, \varphi_{E_+})$) that connects the source and the target states $|A\rangle$ and $|B\rangle$ on the Bloch sphere.

As mentioned earlier, the essential prerequisite for achieving speedups in quantum searching is interference of quantum probability amplitudes [47, 48]. This occurs in both Grover's original quantum search algorithm [26] and in the Farhi-Gutmann continuous version of Grover's algorithm [41]. Indeed, as pointed out by Lloyd in Ref. [27], Grover arrived at the formulation of his quantum search algorithm inspired by the interference of classical waves emitted by an array of antennae.

From an explicit viewpoint, consider a quantum state $|\psi\rangle$ written as the superposition of two normalized quantum states $|A\rangle$ and $|B\rangle$ with complex probability amplitudes $a \stackrel{\text{def}}{=} |a| e^{i\varphi_a}$ and $b \stackrel{\text{def}}{=} |b| e^{i\varphi_b}$, respectively, with φ_a and φ_b in \mathbb{R} . Furthermore, let us assume that $\langle A|B\rangle = \langle B|A\rangle^* \stackrel{\text{def}}{=} |\langle A|B\rangle| e^{i\varphi_{AB}}$ with $\varphi_{AB} \in \mathbb{R}$. Then, the interference law of probability amplitudes a and b can be expressed in terms of their corresponding probabilities calculated by taking a modulus squared of the probability amplitudes. After some simple algebra in which we consider the inner product of $|\psi\rangle$ with itself, the quantum interference law becomes

$$p_{a+b} = p_a + p_b + 2\sqrt{p_a p_b} |\langle A|B\rangle| \cos[\varphi_{AB} - (\varphi_a - \varphi_b)], \quad (46)$$

where $p_{a+b} \stackrel{\text{def}}{=} \langle \psi|\psi\rangle$, $p_a \stackrel{\text{def}}{=} |a|^2$, and $p_b \stackrel{\text{def}}{=} |b|^2$. In Eq. (46), $|\langle A|B\rangle|$ can be viewed as $\cos(\theta_{AB}^{\text{Bloch}}/2)$ with $\theta_{AB}^{\text{Bloch}}$ being the geodesic distance on the Bloch sphere between the states $|A\rangle$ and $|B\rangle$, while $\varphi_a - \varphi_b$ is the absolute phase difference between the interfering probability amplitudes a and b . Interestingly, we remark the contribution of $\langle A|B\rangle \stackrel{\text{def}}{=} |\langle A|B\rangle| e^{i\varphi_{AB}}$ with the interference term $|\langle A|B\rangle| \cos[\varphi_{AB} - (\varphi_a - \varphi_b)]$ into the expression of the total probability p_{a+b} in Eq. (46).

Considering Eqs. (44), (45), and (46), we note that $\langle A|B\rangle \stackrel{\text{def}}{=} |\langle A|B\rangle| e^{i\varphi_{AB}}$ corresponds to $j_{xy} \stackrel{\text{def}}{=} |j_{xy}| e^{i\beta_{xy}}$. In particular, we get

$$\frac{|J_{xy}|}{\sqrt{J_{xx}}\sqrt{J_{yy}}} \stackrel{\text{def}}{=} |j_{xy}| \leftrightarrow \cos\left(\frac{\theta_{AB}^{\text{Poincaré}}}{2}\right) \leftrightarrow \cos\left(\frac{\theta_{AB}^{\text{Bloch}}}{2}\right) \stackrel{\text{def}}{=} \frac{|\langle A|B\rangle|}{\sqrt{\langle A|A\rangle}\sqrt{\langle B|B\rangle}}. \quad (47)$$

Eq. (47) is especially relevant since the degree of correlation of the electric vibrations ($|j_{xy}|$) viewed in terms of the angular separation on the Poincaré sphere ($\theta_{AB}^{\text{Poincaré}}$) can be regarded as corresponding to the geodesic distance on the Bloch sphere ($\theta_{AB}^{\text{Bloch}}$). In the analysis carried out in our paper, both $\cos(\theta_{AB}^{\text{Bloch}}/2)$ and $|j_{xy}|$ played a major role in the proposed definitions of quantum geometric efficiency $\eta_{\text{QM}} \stackrel{\text{def}}{=} s_0/s$ and classical optical efficiency $\eta_{\text{opt}} \stackrel{\text{def}}{=} |j_{xy}|/P$.

In summary, we have discussed the link between propagation of light with maximal degree of coherence and optimal-speed quantum propagation by performing a punctual comparative analysis of geometric flavor. The emergence of this formal analogy is physically motivated by the existence of a key physical phenomenon that underlies both types of evolutions at their best, i.e., interference. This link among $|j_{xy}|$, $\theta_{AB}^{\text{Poincaré}}$, and $\theta_{AB}^{\text{Bloch}}$ in Eq. (47) that emerges while thinking of interference of classical waves (classical optics) and interference of probability amplitudes (quantum mechanics) should be kept in mind as a constant (hidden) theme underlying our discussion in the main paper.

VI. CONCLUDING REMARKS

In this paper, we identified and discussed in a quantitative manner a link between the geometry of time-independent optimal-speed Hamiltonian quantum evolutions on the Bloch sphere and the geometry of intensity-preserving propagation of light with maximal degree of coherence on the Poincaré sphere.

Specifically, we carried out a detailed comparative analysis between the quantum and optical scenarios. In the quantum case, we focused on the main constraint equations (Eqs. (2) and (13)) leading to the construction of the

optimal unitary evolution operator $e^{-\frac{i}{\hbar}HT_{AB}}$ (that is, a rotation of a Bloch vector on the Bloch sphere) with the optimal Hamiltonian given in Eqs. (11) and (19). In the optical case, similarly, we focused on the main constraint equations (Eqs. (34) and (35)) leading to the construction of the optimal Mueller matrix $M_{\text{ROT}}(\varphi_{\text{opt}})$ (see Eq. (39) with φ_{opt} in Eq.(40). This Mueller matrix acts on a Stokes vector on the Poincaré sphere (see Eq. (38)) and leads to the propagation of light with maximal degree of coherence in analogy to the geodesic path defined in Eq. (20) and generated by the Hamiltonian in Eq. (19). In particular, in Table I we presented an explicit correspondence between the main quantum and optical quantities that enter the two phenomena. In Table II, we pointed out the two main constraint relations that specify the two physical scenarios. Finally, in Table III, we concluded with the correspondence between axes and angles of rotations that specify the two optimal operations yielding unit quantum geometric efficiency and classical optical efficiency, respectively.

Our main achievement in this paper is bringing to light this fascinating analogy between optimal-speed quantum evolutions and polarized light propagation with maximal degree of coherence. This link was never noticed before and, to the best of our knowledge, it constitutes a new connection between the quantum physics of two-level systems and classical polarization optics. To a certain extent, we think that our investigation is not only relevant from a pure theoretical perspective, it can also be regarded (in retrospect) as providing a sort of conceptual and quantitative geometric background underlying Grover's powerful intuition about constructing a quantum search scheme by mimicking interference of classical waves [27]. For the time being, its interest remains foundational in flavor. However, we shall be seeking ways to exploit this formal theoretical analogy for more practical purposes in future investigations concerning the construction of quantum search algorithms.

Acknowledgments

C.C. is grateful to the United States Air Force Research Laboratory (AFRL) Summer Faculty Fellowship Program for providing support for this work. S.R. acknowledges support from the National Research Council Research Associate Fellowship program (NRC-RAP). P.M.A. acknowledges support from the Air Force Office of Scientific Research (AFOSR). Any opinions, findings and conclusions or recommendations expressed in this material are those of the author(s) and do not necessarily reflect the views of the Air Force Research Laboratory (AFRL).

-
- [1] U. Fano, *A Stokes-parameter technique for the treatment of polarization in quantum mechanics*, Phys. Rev. **93**, 121 (1954).
 - [2] M. A. Nielsen and I. L. Chuang, *Quantum Computation and Quantum Information*, Cambridge University Press (2000).
 - [3] M. Born and E. Wolf, *Principles of Optics*, Cambridge University Press (2003).
 - [4] S. Pancharatnam, *Generalized theory of interference, and its applications*, Proc. Ind. Acad. Sci. **A44**, 247 (1956).
 - [5] M. V. Berry, *Quantal phase factors accompanying adiabatic changes*, Proc. R. Soc. Lond. **A392**, 45 (1984).
 - [6] P. K. Aravind, *A simple proof of Pancharatnam's theorem*, Optics Communications **P4**, 191 (1992).
 - [7] M. V. Berry, *The adiabatic phase and Pancharatnam's phase for polarized light*, J. Mod. Opt. **34**, 1401 (1987).
 - [8] J. Samuel and R. Bhandari, *General setting for Berry's phase*, Phys. Rev. Lett. **60**, 2339 (1988).
 - [9] R. Y. Chiao and Y.-S. Wu, *Manifestation of Berry's topological phase for the photon*, Phys. Rev. Lett. **57**, 933 (1986).
 - [10] T. F. Jordan, *Direct calculation of the Berry phase for spins and helicities*, J. Math. Phys. **28**, 1759 (1987).
 - [11] H. Moya-Cessa, J. R. Moya-Cessa, J. E. A. Landgrave, G. Martinez-Niconoff, A. Perez-Leija, and A. T. Friberg, *Degree of polarization and quantum-mechanical purity*, J. Eur. Opt. Soc. Rap. Public. **3**, 08014 (2008).
 - [12] O. Gamel and D. F. V. James, *Measures of quantum state purity and classical degree of polarization*, Phys. Rev. **A86**, 033830 (2012).
 - [13] C. M. Bender, D. C. Brody, H. F. Jones, and B. K. Meister, *Faster than Hermitian quantum mechanics*, Phys. Rev. Lett. **98**, 040403 (2007).
 - [14] A. Mostafazadeh, *Hamiltonians generating optimal-speed evolutions*, Phys. Rev. **A79**, 014101 (2009).
 - [15] D. C. Brody and D. W. Hook, *On optimum Hamiltonians for state transformations*, J. Phys. A: Math. Gen. **39**, L167 (2006).
 - [16] D. C. Brody and D. W. Hook, *On optimum Hamiltonians for state transformation*, J. Phys. A: Math. Theor. **40**, 10949 (2007).
 - [17] D. C. Brody, *Elementary derivation for passage times*, J. Phys. A: Math. Gen. **36**, 5587 (2003).
 - [18] J. Anandan and Y. Aharonov, *Geometry of quantum evolution*, Phys. Rev. Lett. **65**, 1697 (1990).
 - [19] C. Cafaro, S. Ray, and P. M. Alsing, *Geometric aspects of analog quantum search evolutions*, Phys. Rev. **A102**, 052607 (2020).
 - [20] E. Wolf, *Coherence properties of partially polarized electromagnetic radiation*, Il Nuovo Cimento **13**, 1180 (1959).
 - [21] C. Cafaro, *Geometric algebra and information geometry for quantum computational software*, Physica **A470**, 154 (2017).
 - [22] C. Cafaro and P. M. Alsing, *Theoretical analysis of a nearly optimal analog quantum search*, Physica Scripta **94**, 085103 (2019).

- [23] C. Cafaro and P. M. Alsing, *Continuous-time quantum search and time-dependent two-level quantum systems*, Int. J. Quantum Information **17**, 1950025 (2019).
- [24] S. Gassner, C. Cafaro, and S. Capozziello, *Transition probabilities in generalized quantum search Hamiltonian evolutions*, Int. J. Geom. Meth. Mod. Phys. **17**, 2050006 (2020).
- [25] C. Cafaro, D. Felice, and P. M. Alsing, *Quantum Groverian geodesic paths with gravitational and thermal analogies*, Eur. Phys. J. Plus **135**, 900 (2020).
- [26] L. K. Grover, *Quantum mechanics helps in searching for a needle in a haystack*, Phys. Rev. Lett. **79**, 325 (1997).
- [27] S. Lloyd, *Quantum search without entanglement*, Phys. Rev. **A61**, 010301(R) (1999).
- [28] Note that our Eq. (11) fixes a typographical error that appears in Eq. (6) of Ref. [13]. As a cross check, we also verified that our Hamiltonian in Eq. (11) satisfies the correct maximal energy dispersion relation $\Delta E = \Delta E_{\max} \stackrel{\text{def}}{=} (E_+ - E_-)/2 = E_0/2$ with $E_+ - E_- \stackrel{\text{def}}{=} E_0 = \text{fixed}$.
- [29] Observe that our Eq. (18) fixes a typographical error that appears in Eq. (12) of Ref. [14]. As a cross check, we also verified that our Hamiltonian in Eq. (18) satisfies the correct maximal energy dispersion relation given by $\Delta E = \Delta E_{\max} \stackrel{\text{def}}{=} (E_+ - E_-)/2 = E$ with $E_+ = -E_- \stackrel{\text{def}}{=} E$.
- [30] S. Chandrasekhar, *Radiative Transfer*, Clarendon Press (1950).
- [31] E. Collett, *The description of polarization in classical physics*, Am. J. Phys. **36**, 713 (1968).
- [32] M. J. Walker, *Matrix calculus and the Stokes parameters of polarized radiation*, Am. J. Phys. **22**, 170 (1954).
- [33] R. C. Jones, *A new calculus for the treatment of optical systems. I. Description and discussion of the calculus*, J. Opt. Soc. Am. **31**, 488 (1941); R. C. Jones, *A new calculus for the treatment of optical systems. IV*, J. Opt. Soc. Am. **32**, 486 (1942).
- [34] H. Mueller, *The foundation of optics*, J. Opt. Soc. Am. **38**, 661 (1948).
- [35] G. Stokes, *On the composition and resolution of streams of polarized light from different sources*, Trans. Cambridge Phil. Soc. **9**, 399 (1852).
- [36] F. Perrin, *Polarization of light scattered by isotropic opalescent media*, J. Chem. Phys. **10**, 415 (1942).
- [37] H. Poincaré, *Traité de la Lumière*, Paris **2**, 165 (1892).
- [38] N. Wiener, *Generalized harmonic analysis*, Acta Math. **55**, 117 (1930).
- [39] S. Baskal, Y. S. Kim, and M. E. Noz, *Mathematical Devices for Optical Sciences*, IOP Publishing Ltd (2019).
- [40] R. A. Chipman, W.-S. Tiffany Lam, and G. Young, *Polarized Light and Optical Systems*, CRC Press (2019).
- [41] E. Farhi and S. Gutmann, *Analog analogue of a digital quantum computation*, Phys. Rev. **A57**, 2403 (1998).
- [42] L. Mandel, *Coherence and indistinguishability*, Optics Letters **16**, 1882 (1991).
- [43] R. Cleve, A. Ekert, L. Henderson, C. Macchiavello, and M. Mosca, *On quantum algorithms*, Complexity **4**, 33 (1998).
- [44] R. Cleve, A. Ekert, C. Macchiavello, and M. Mosca, *Quantum algorithms revisited*, Proc. Roy. Soc. Lond. **A454**, 339 (1998).
- [45] E. Wolf, *Introduction to the Theory of Coherence and Polarization of Light*, Cambridge University Press (2007).
- [46] R. Loudon, *The Quantum Theory of Light*, Oxford University Press (2000).
- [47] A. Ekert and R. Jozsa, *Quantum computation and Shor's factoring algorithm*, Rev. Mod. Phys. **68**, 733 (1996).
- [48] A. Galindo and M. A. Martin-Delgado, *Information and computation: classical and quantum aspects*, Rev. Mod. Phys. **74**, 347 (2002).
- [49] R. C. Jones, *A new calculus for the treatment of optical systems V. A more general formulation, and description of another calculus*, J. Opt. Soc. Am. **37**, 107 (1947).
- [50] A. Z. Goldberg, *Quantum theory of polarimetry: From quantum operations to Mueller matrices*, Phys. Rev. Research **2**, 023038 (2020).
- [51] D. G. Anderson and R. Barakat, *Necessary and sufficient conditions for a Mueller matrix to be derivable from a Jones matrix*, J. Opt. Soc. Am. **A11**, 2305 (1994).
- [52] S.-Y. Lu and R. A. Chipman, *Interpretation of Mueller matrices based on polar decomposition*, J. Opt. Soc. Am. **A13**, 1106 (1996).
- [53] L. H. Ryder, *Quantum Field Theory*, Cambridge University Press (1996).
- [54] E. P. Wigner, *Group Theory and its Applications to Quantum Mechanics*, Academic Press, New York (1959).
- [55] S. R. Cloude, *Group theory and polarisation algebra*, Optik **75**, 26 (1986).
- [56] T. Qureshi, *Coherence, interference and visibility*, Quanta **8**, 24 (2019).
- [57] A. Carlini, A. Hosoya, T. Koike, and Y. Okudaira, *Time-optimal quantum evolution*, Phys. Rev. Lett. **96**, 060503 (2006).
- [58] X. Wang, M. Allegra, K. Jacobs, S. Lloyd, C. Lupo, and M. Mohseni, *Quantum brachistochrone curves as geodesics: Obtaining accurate minimum-time protocols for the control of quantum systems*, Phys. Rev. Lett. **114**, 170501 (2015).

Appendix A: Mueller matrices

In this Appendix, we provide further details on the Mueller matrices mentioned in subsection B of Section III. Furthermore, we devote special emphasis on their relation with the Jones matrices. Finally, we emphasize how points on the surface of the Poincaré sphere are rotated by means of specific types of Mueller matrices.

In the traditional approach to polarization optics, the light propagates along the \hat{z} -axis and one considers the electric vector field components along the \hat{x} - and \hat{y} -directions. The polarization state is determined by the amplitude

ratio and phase difference of the electric field components. Therefore, polarization can be modified either by changing the amplitudes or by tuning the relative phases, or both. Within the Jones calculus [33, 49], the Jones vector in \mathbb{C}^2 represents the polarized light by means of the amplitude and the phase of the electric field in the \hat{x} - and \hat{y} -directions. Furthermore, linear optical elements (for instance, beam splitters, lenses, and mirrors) are represented by 2×2 Jones matrices. Within the Mueller calculus [34], employing the concepts of Stokes parameters and Poincaré sphere, the change of polarization due to the interaction of light with an optical device can be described by the action of a 4×4 matrix that represents a linear transformation acting upon a 4×1 matrix corresponding to the Stokes vector. Within the Mueller calculus, there are three fundamental optical elements: wave plates, rotators, and polarizers. A wave plate and a rotator produce phase shifts and rotations of the Stokes vector, respectively. They are described by unitary matrices since they do not change the intensity of the light. Polarizers cause anisotropic attenuation and do change the intensity of light passing through them. Therefore, unlike wave plates and rotators, they are described by nonunitary matrices. The matricial representation of optical devices is very useful. Indeed, the composite effect of a series of optical devices crossed by a light beam is represented by the product of the matrices corresponding to the various optical elements in the series. Mueller matrices can be grouped into two main categories [50]: Nondepolarizing and depolarizing Mueller matrices. Nondepolarizing Mueller matrices can modify the degree of polarization of partially polarized light. However, they do not change the degree of polarization of perfectly polarized light. Depolarizing Mueller matrices, instead, while maintaining the total intensity of the light beam, do reduce the degree of polarization of completely polarized light. Furthermore, nondepolarizing Mueller matrices have equivalent Jones matrices. On the other hand, depolarizing Mueller matrices have no equivalent Jones matrices. For a discussion on necessary and sufficient conditions for a Mueller matrix to be derivable from a Jones matrix, we refer to Ref. [51]. Interestingly, it is possible to show that any Mueller matrix can be decomposed into a sequence of three matrix factors [52]: a diattenuator, followed by a retarder, then followed by a depolarizer. Diattenuators and retarders are described by Hermitian Jones matrices and change only the amplitudes of the components of the electric field vector. A polarizer is an example of a diattenuator. Retarders, instead, are described by unitary Jones matrices and change only the phases of components of the electric field vector. A wave plate is an example of a retarder. As mentioned earlier, there are Mueller matrices with no corresponding Jones matrices. However, it turns out that any Jones matrix J acting on the electric field \vec{E} can be transformed into the corresponding Mueller matrix M given by $M \stackrel{\text{def}}{=} A(J \otimes J^*)A^{-1}$, where “ $*$ ” and “ \otimes ” denote the complex conjugate and the tensor product, respectively. Moreover, A is a 4×4 matrix defined as,

$$A \stackrel{\text{def}}{=} \begin{pmatrix} 1 & 0 & 0 & 1 \\ 1 & 0 & 0 & -1 \\ 0 & 1 & 1 & 0 \\ 0 & -i & i & 0 \end{pmatrix}. \quad (\text{A1})$$

Observe that the four rows $\{R_A^i\}_{1 \leq i \leq 4}$ of A in Eq. (A1) are given by the coefficients of the identity matrix I and the three Pauli matrices $\{\sigma_x, \sigma_y, \sigma_z\}$ with $R_A^1 \leftrightarrow I$, $R_A^2 \leftrightarrow \sigma_z$, $R_A^3 \leftrightarrow \sigma_x$, and $R_A^4 \leftrightarrow \sigma_y$. It is well-known that there is a two-to-one homomorphism between the complex special unitary group $SU(2)$ and the real group of three-dimensional pure rotations $O^+(3)$ [53],

$$SU(2) \ni e^{i\vec{\sigma} \cdot \hat{n} \frac{\theta}{2}} \leftrightarrow e^{i\vec{J} \cdot \hat{n} \theta} \in O^+(3). \quad (\text{A2})$$

In Eq. (A2), \hat{n} denotes the axis of rotation, θ is the angle of rotation, $\vec{\sigma} \stackrel{\text{def}}{=} (\sigma_1, \sigma_2, \sigma_3)$ is the Pauli matrix vector, and $\vec{J} \stackrel{\text{def}}{=} (J_1, J_2, J_3)$ is the generator vector for $O^+(3)$. Interestingly, it can be shown that the matrix coefficients R_{ij} of any rotation matrix R in $O^+(3)$ can be recast as [54],

$$R_{ij} = \frac{1}{2} \text{tr}(U^\dagger \cdot \sigma_i \cdot U \cdot \sigma_j), \quad (\text{A3})$$

where U is a two-dimensional unitary matrix with determinant equal to one specified by three free (real) parameters. From Eqs. (A2) and (A3), we note there is a global topological difference between $SU(2)$ and $O^+(3)$. For example, increasing the angle θ by 2π in Eq. (A2), we get $U \rightarrow -U$ in $SU(2)$ while $R \rightarrow R$ in $O^+(3)$. Therefore, both U and $-U$ in $SU(2)$ correspond to the same R in $O^+(3)$. Thus, there exists a two-to-one mapping of elements of $SU(2)$ onto $O^+(3)$. Exploiting the $SU(2)$ - $O^+(3)$ homomorphism, it happens that to a $SU(2)$ matrix U acting on the vector field \vec{E} there corresponds a 4×4 Mueller matrix viewed as an augmented form of a $O^+(3)$ matrix R [55],

$$M \stackrel{\text{def}}{=} \begin{pmatrix} 1_{1 \times 1} & O_{1 \times 3} \\ O_{3 \times 1} & R_{3 \times 3} \end{pmatrix}, \quad (\text{A4})$$

where the coefficients M_{ij} of the matrix M are given by,

$$M_{ij} \stackrel{\text{def}}{=} \frac{1}{2} \text{tr} (U^\dagger \cdot \Xi_i \cdot U \cdot \Xi_j), \quad (\text{A5})$$

with $\Xi \stackrel{\text{def}}{=} (I, \sigma_z, \sigma_x, \sigma_y)$. For completeness, we remark that Eq. (A5) can also be extended by considering arbitrary complex (scattering) matrices U_{complex} in place of $SU(2)$ matrices. In this case, the effect of the Mueller matrix with coefficients $M_{ij} \stackrel{\text{def}}{=} 1/2 \text{tr} (U_{\text{complex}}^\dagger \cdot \Xi_i \cdot U_{\text{complex}} \cdot \Xi_j)$ is to combine a rotation of the Stokes vector with a change of its length (which, in turn, corresponds to a change in the degree of polarization). For more details on polarization algebra with Mueller matrices, we refer to Ref. [55].

Appendix B: Degree of coherence of partially polarized waves

In this Appendix, we use the Poincaré sphere formalism to describe the behavior of the modulus $|j_{xy}|$ of the complex degree of coherence j_{xy} of partially polarized light beams in terms of the ellipticity and orientation angles. Appendix B helps better understanding the content of subsection B of Section III with regard to partially polarized light waves with $P < 1$.

Partially polarized waves can be regarded as points that are inside the Poincaré sphere of radius I_{tot} (i.e., the total intensity of the wave) and at a distance I_{pol} (i.e., the intensity of the polarized part of the wave) from the origin of the sphere itself. Using the Stokes parameters $\{S_0, S_1, S_2, S_3\}$, we note that the degree of polarization P and $|j_{xy}|$ can be recast as,

$$P = \frac{(S_1^2 + S_2^2 + S_3^2)^{1/2}}{S_0}, \text{ and } |j_{xy}| = \left(\frac{S_2^2 + S_3^2}{S_0^2 - S_1^2} \right)^{1/2}, \quad (\text{B1})$$

respectively. From Eq. (B1), we have that if $S_0^2 = S_1^2 + S_2^2 + S_3^2$ then $P = |j_{xy}| = 1$. Instead, if $S_0^2 > S_1^2 + S_2^2 + S_3^2$ then $P < 1$ and $|j_{xy}| \leq P$. Furthermore, using the two relations in Eq. (B1) along with setting $S_0 \stackrel{\text{def}}{=} I_{\text{tot}}$, $S_1 \stackrel{\text{def}}{=} I_{\text{pol}} \cos(2\beta) \cos(2\chi)$, $S_2 \stackrel{\text{def}}{=} I_{\text{pol}} \cos(2\beta) \sin(2\chi)$, and $S_3 \stackrel{\text{def}}{=} I_{\text{pol}} \sin(2\beta)$, we get

$$|j_{xy}| = |j_{xy}|(\beta, \chi; P) \stackrel{\text{def}}{=} P \left[\frac{1 - \cos^2(2\beta) \cos^2(2\chi)}{1 - P^2 \cos^2(2\beta) \cos^2(2\chi)} \right]^{1/2}, \quad (\text{B2})$$

where $P \stackrel{\text{def}}{=} I_{\text{pol}}/I_{\text{tot}}$, $-\pi/4 < \beta \leq \pi/4$, and $0 \leq \chi < \pi$. Finally, we note from Eq. (B2) that for a given value of $P < 1$ and for any value of the ellipticity angle $\beta \in (-\pi/4, \pi/4]$, the maximum of $|j_{xy}|$ equals P and is achieved when the orientation angle χ equals $\pi/4$.

Appendix C: Parametrizations of qubits and polarization states

In this Appendix, we report for completeness some mathematical details on the parametrization of qubits and polarization states viewed as points on the Bloch sphere and the Poincaré sphere, respectively. These details help comprehending the schematic depictions in Fig. 1.

In terms of the computational basis vectors $|0\rangle$ and $|1\rangle$, a normalized qubit is a point on the Bloch sphere that can be parametrized as

$$|\psi(\theta, \varphi)\rangle \stackrel{\text{def}}{=} \cos\left(\frac{\theta}{2}\right) |0\rangle + e^{i\varphi} \sin\left(\frac{\theta}{2}\right) |1\rangle, \quad (\text{C1})$$

with $0 \leq \theta \leq \pi$ and $0 \leq \varphi < 2\pi$. The Bloch sphere metric is given by $ds_{\text{Bloch}}^2 \stackrel{\text{def}}{=} d\hat{n}_B \cdot d\hat{n}_B = d\theta^2 + \sin^2(\theta) d\varphi^2$ with $\hat{n}_B \stackrel{\text{def}}{=} \langle \psi(\theta, \varphi) | \vec{\sigma} | \psi(\theta, \varphi) \rangle = (\sin\theta \cos\varphi, \sin\theta \sin\varphi, \cos\theta)$ and $\vec{\sigma} \stackrel{\text{def}}{=} (\sigma_x, \sigma_y, \sigma_z)$ being the usual vector of Pauli matrices.

In terms of the orthonormal circular basis states \hat{e}_{RC} (right circular) and \hat{e}_{LC} (left circular), the general equation of a normalized state of polarization $\hat{e}(\beta, \chi)$ viewed as a point on the Poincaré sphere is given by

$$\hat{e}(\beta, \chi) \stackrel{\text{def}}{=} \frac{\cos(\beta) + \sin(\beta)}{\sqrt{2}} \hat{e}_{\text{RC}} + e^{i2\chi} \frac{\cos(\beta) - \sin(\beta)}{\sqrt{2}} \hat{e}_{\text{LC}}, \quad (\text{C2})$$

with $-\pi/4 < \beta \leq \pi/4$ and $0 \leq \chi < \pi$. The Poincaré metric is given by $ds_{\text{Poincaré}}^2 \stackrel{\text{def}}{=} d\hat{n}_P \cdot d\hat{n}_P = 4 [d\beta^2 + \cos^2(2\beta) d\chi^2]$ where $\hat{n}_P \stackrel{\text{def}}{=} \langle \hat{e}(\beta, \chi), \vec{\sigma} \hat{e}(\beta, \chi) \rangle_{\mathbb{C}} = (\cos(2\beta) \cos(2\chi), \cos(2\beta) \sin(2\chi), \sin(2\beta))$, with $\langle \cdot, \cdot \rangle_{\mathbb{C}}$ denoting the usual complex inner product. From Eq. (C2), note that points on the poles specify circularly polarized light, $\hat{e}_{\text{RC}} \stackrel{\text{def}}{=} \hat{e}(\pi/4, 0)$ and $\hat{e}_{\text{LC}} \stackrel{\text{def}}{=} \hat{e}(-\pi/4, 0)$. Furthermore, points on the equator correspond to linearly polarized light, $\hat{e}_{\text{VL}} \stackrel{\text{def}}{=} \hat{e}(0, \pi/2)$ (vertical linear) and $\hat{e}_{\text{HL}} \stackrel{\text{def}}{=} \hat{e}(0, 0)$ (horizontal linear). Ignoring an overall phase, we remark that $\hat{e}_{\text{RC}} \stackrel{\text{def}}{=} (\hat{e}_{\text{HL}} - i\hat{e}_{\text{VL}})/\sqrt{2}$ and $\hat{e}_{\text{LC}} \stackrel{\text{def}}{=} (\hat{e}_{\text{HL}} + i\hat{e}_{\text{VL}})/\sqrt{2}$. Finally, the remaining points on the Poincaré sphere represent other elliptical polarization states.

Appendix D: Interference effects in propagation of light, quantum searching, and optimal-speed quantum evolutions

In this Appendix, we present some comments on the role played by interference effects in light propagation, quantum searching, and optimal-speed quantum evolutions. These remarks integrate those presented in Section V.

In the study of propagation of light, coherent sources are required for producing interference patterns. In particular, interference of light beams appear in the calculation of the total intensity of the resultant beam obtained in terms of a superposition of two coherent beams. In this context, the objective is to obtain propagation of light with maximal degree of coherence. Maximization of the absolute value of the complex degree of coherence, interpreted as a measure of the degree of correlation of the electric vibrations of the wave, yield more visible interference patterns. Indeed, the degree of coherence establishes in a formal manner how distinctly visible is the interference pattern [56]. We note that to have a nonzero degree of coherence, the coherency matrix has to have nonvanishing off-diagonal terms [3, 20]. This observation becomes especially interesting when we recall that quantum computation derives its power from entanglement and quantum interference. In particular, the degree of interference in a N -qubit register is specified by the coherences, that is, the off-diagonal elements ρ_{lm} with $l \neq m$ of the density operator in the computation basis. Therefore, the role played by coherences in quantifying the degree of quantum interference viewed as a source of power for quantum computing can be grasped in a straightforward manner [47]. These considerations lead us to the following question: Where does the phenomenon of quantum interference manifest itself in the quantum computational tasks considered in our paper?

In Grover's digital quantum search algorithm [26], the interference of quantum probability amplitudes appears in the calculation of the transition probability from the (known) source state to the (unknown) target state. Indeed, in quantum searching, the goal is to achieve unit transition probability (defined as the modulus squared of the quantum overlap between the target state and the source state acted upon by a number of iterations of Grover's operator) with the smallest number of iterations of Grover's operator. More specifically, quantum searching can be explained as inducing a desired relative phase between two eigenvectors of Grover's operator to yield constructive interference on the target state (that is, use quantum interference to nudge up the searched state) and destructive interference on the remaining states [43, 44]. In the Farhi-Gutmann analog quantum search evolution viewed as the continuous-time version of Grover's search scheme [41], the interference of quantum probability amplitudes emerges in the computation of the transition probability from the (known) source state to the (unknown) target state. The goal there is to achieve unit transition probability in the shortest amount of time. The Farhi-Gutmann search Hamiltonian specifies the dynamical process of quantum interference which, in turn, allows one to evolve from the source state to the target state in the smallest possible time by modifying the explored intermediate superpositions of quantum states in a suitably prescribed manner so that time optimality [57, 58] is achieved. Finally, in the optimal-speed quantum Hamiltonian evolutions [13, 14], interference of quantum probability amplitudes can be identified in the maximization of the energy uncertainty (that is, the dispersion of the Hamiltonian operator). This maximization is required in order to evolve from a (known) source state to a (known) target state with optimal-speed (that is, the maximum energy uncertainty and the smallest travel time). The optimal-speed time-independent Hamiltonian specifies, via its eigenvector decomposition, the process of quantum interference. The latter, in turn, allows us to transition from the source to the target states in the shortest possible time by navigating through a path of quantum states while preserving maximal energy uncertainty. Interestingly, we pointed out the correspondence between intensity of light and energy of the quantum system in the constraint equations that appear in Table II.